Infrared Emitters and Detectors Data Book 1997

TEMIC
Semiconductors

Contents

General Information 1
Alphanumeric Index 1
Selector Guide 2
Infrared Emitting Diodes 2
Detectors 4
Conventions Used in Presenting Technical Data 7
Nomenclature for Semiconductor Devices According to Pro Electron 7
TEMIC Type Designation Code 8
Symbols and Terminology 9
Data Sheet Structure 17
Physics and Technology 18
Emitters 18
UV, Visible, and Near IR Silicon Photodetectors 21
Measurement Techniques 31
Introduction 31
Dark and Light Measurements 31
Switching Characteristics 36
Component Construction 37
Tape and Reel Standards 38
Packing 38
Order Designation 38
Taping of SMT-Devices 44
Assembly instructions 47
General 47
Soldering instructions 47
Heat Removal 49
Cleaning 50
Warning 50
Quality Information 51
General Quality Flow Chart Diagram 52
Production Flow Chart Diagram 53
Qualification and Release 54
Statistical Methods for Prevention 54
Reliability 55
Average Outgoing Quality (AOQ) 55
Early Failure Rate (EFR) 55
Long-Term Failure Rate (LFR) 55
Confidence Level 55
Mean Time to Failure (MTTF) 56
Activation Energy 57
Degradation of IREDs 58
Safety 58
Data Sheets 59
Infrared Emitters 61
Photodetectors 203
Addresses 419

Conventions Used in Presenting Technical Data

Nomenclature for Semiconductor Devices According to Pro Electron

The type number of semiconductor devices consists of:

Two letters followed by a serial number

For example:

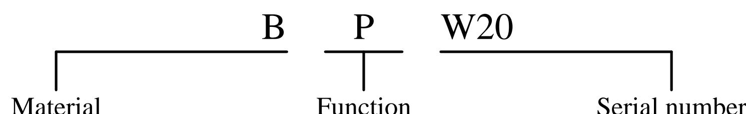

The **first letter** indicates the material used for the active part of the device.

A GERMANIUM
(Materials with a bandgap 0.6–1.0 eV) [1)]

B SILICON
(Materials with a bandgap 1.0–1.3 eV) [1)]

C GALLIUM-ARSENIDE
(Materials with a bandgap > 1.3 eV) [1)]

R COMPOUND MATERIALS
(For instance Cadmium-Sulphide)

The **second letter** indicates the circuit function:

A DIODE: detection, switching, mixer

B DIODE: variable capacitance

C TRANSISTOR: low power, audio frequency

D TRANSISTOR: power, audio frequency

E DIODE: tunnel

F TRANSISTOR: low power, high frequency

G DIODE: oscillator, miscellaneous

H DIODE: magnetic sensitive

K HALL EFFECT DEVICE: in an open magnetic circuit

L TRANSISTOR: power, high frequency

M HALL EFFECT DEVICE: in a closed magnetic circuit

N PHOTO COUPLER

P DIODE: radiation sensitive

Q DIODE: radiation generating

R THYRISTOR: low power

S TRANSISTOR: low power, switching

T THYRISTOR: power

U TRANSISTOR: power, switching

X DIODE: multiplier, e.g. varactor, step recovery

Y DIODE: rectifying, booster

Z DIODE: voltage reference or voltage regulator. transient suppressor diode

The **serial number** consists of:

- Three figures, running from 100 to 999, for devices primarily intended for consumer equipment
- One letter (Z, Y, X, etc.) and two figures, running from 10 to 99, for devices primarily intended for professional equipment

A version letter can be used to indicate a deviation of a single characteristic, either electrically or mechanically. The letter never has a fixed meaning, the only exception being the letter R, indicating reversed voltage, i.e. collector to case.

[1)] The materials mentioned are examples

TEMIC Type Designation Code

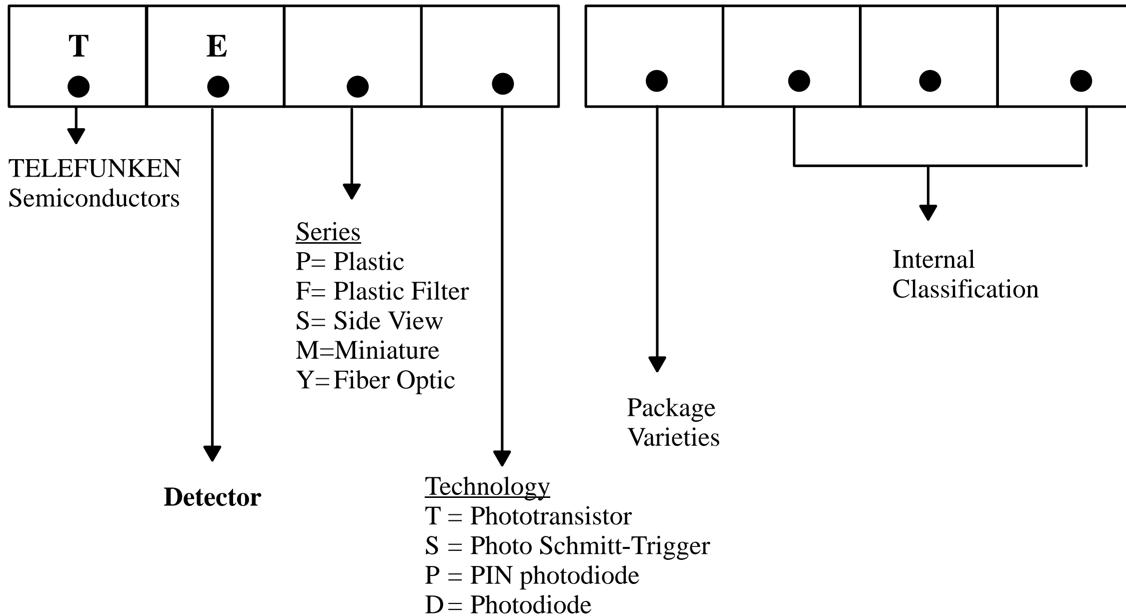

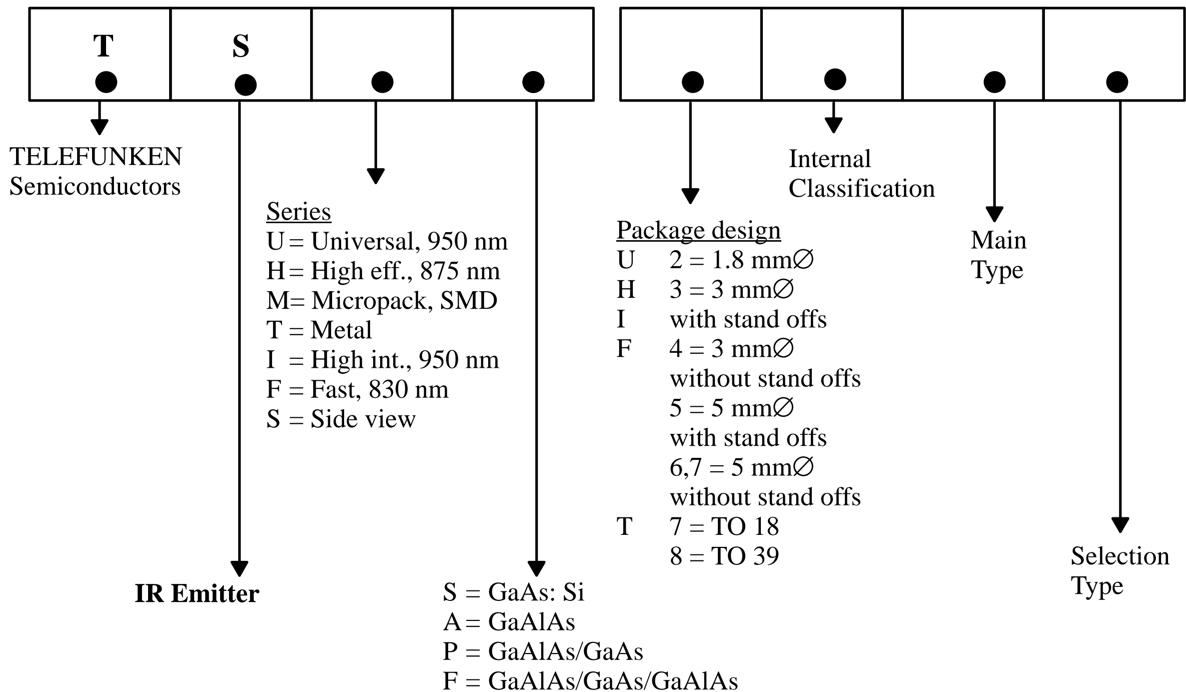

Symbols and Terminology

Symbols alphabetically

A
Anode, anode terminal

A
Radiant sensitive area
That area which is radiant sensitive for a specified range

a
Distance between the emitter (source) and the detector

B
Base, base terminal

C
Capacitance

C
Cathode, cathode terminal
Collector, collector terminal

°C
Celsius
Unit of the centigrade scale; can also be used (beside K) to express temperature changes
Symbols: T, ΔT
T (°C) = T (K) - 273

C_{CEO}
Collector-emitter capacitance
Capacitance between the collector and the emitter with open base

cd
Candela
SI unit of luminous intensity I_v

C_D
Diode capacitance
Total capacitance effective between the diode terminals due to case, junction and parasitic capacitances

C_j
Junction capacitance
Capacitance due to a pn junction of a diode,
decreases with increasing reverse voltage

E
Emitter, emitter terminal (phototransistor)

E_A
Illumination at standard illuminant A
According to DIN 5033 and IEC 306-1, illumination emitted from a tungsten filament lamp with a color temperature T_f = 2855.6 K which is equivalent to standard illuminant A
Unit: lx (Lux) or klx

$E_{A\ amb}$
Ambient illumination at standard illuminant A

E_e
Irradiance (at a point of a surface)
Quotient of the radiant power incident on an element of the surface containing the point, by the area of that element

$$E_e = \frac{d\Phi_e}{dA}$$

E_v
Illuminance (at a point of a surface)
Quotient of the luminous flux incident on an element of the surface containing the point, by the area of that element

$$E_v = \frac{d\Phi_v}{dA}$$

Unit: lx (Lux) = lm/m^2

f
Frequency
Unit: Hz (Hertz)

f_c
Cut-off frequency – detector devices
The frequency at which the incident radiation generates a photocurrent or a photovoltage 0.707 times the value of radiation at f = 1 kHz

f_s
Switching frequency

I_a
Light current
General: Current which flows through a device due to irradiation/illumination

I_B
Base current

I_{BM}
Base peak current

I_C
Collector current

I_{ca}
Collector light current
Collector current under irradiation (IEC747-5)
Collector current which flows at a specified illumination/irradiation

I_{CEO}
Collector dark current, with open base
Collector-emitter dark current (IEC747-5)
For radiant sensitive devices with open base and without illumination/radiation (E = O)

I_{CM}
Repetitive peak collector current

I_e
Radiant intensity (of a source in a given direction)
Quotient of the radiant power leaving the source propagated in an element of solid angle containing the given direction, by the element of solid angle.
Radiant intensity I_e of emitters is typically measured with an angle ≤ 0.01 sr on mechanical axis or off-axis in the maximum of the irradiation pattern.

$$I_e = \frac{d\Phi_e}{d\Omega}$$

Unit: W/sr, mW/sr

I_F
Continuous forward current
The current flowing through the diode in the direction of lower resistance

I_{FAV}
Average (mean) forward current

I_{FM}
Peak forward current

I_{FSM}
Surge forward current

I_k
Short-circuit current
That value of the current which flows when a photovoltaic cell or a photodiode is short circuited ($R_L \ll R_i$) at its terminals

I_{ph}
Photocurrent (photoelectric current)
That part of the electric current in a photoelectric detector which is produced by the photoelectric effect

I_o
dc output current

I_R
Reverse current, leakage current
Current which flows when reverse bias is applied to a semiconductor junction

I_{ra}
Reverse light current
Reverse current under irradiation (IEC747-5)
Reverse light current which flows due to a specified irradiation/illumination in a photoelectric device

$$I_{ra} = I_{ro} + I_{ph}$$

I_{ro}
Reverse dark current
Dark current (IEC747-5)
Reverse current flowing through a photoelectric device in the absence of irradiation

I_{SB}
Quiescent current

I_{SD}
Supply current in dark ambient

I_{SH}
Supply current in bright ambient

K
Kelvin
The SI unit of temperature T (also called the Kelvin temperature); can also be used for temperature differences (formerly °K)

lm
Lumen

lx
Lux

N.A.
Numerical Aperture
N.A. = sin $\alpha/2$
Term used for the characteristic of sensitivity or intensity angles of fiber optics and objectives

NEP
Noise Equivalent Power

P_{tot}
Total power dissipation

P_v
Power dissipation, general

R_D
Dark resistance

R_F
Feedback resistor

R_i
Internal resistance

R_{is}
Isolation resistance

R_L
Load resistance

R_S
Serial resistance

R_{sh}
The shunt resistance is defined and measured at a voltage of 10 mV forward or reverse, or peak-to-peak

R_{thJA}
Thermal resistance, junction to ambient

R_{thJC}
Thermal resistance, junction to case

S
Sensitivity, absolute
Ratio of the output value Y of a radiant-sensitive device to the input value X of a physical quantity:

$$S = \frac{Y}{X}$$

Unit: A/lx, A/W

$s(\lambda)$
Absolute spectral sensitivity at a wavelength λ
The ratio of the output quantity to the radiant input quantity in the range of wavelengths λ to $(\lambda + d\lambda)$:

$$s(\lambda) = \frac{dy(\lambda)}{dx(\lambda)}$$

e.g., the radiation power $\Phi_e(\lambda)$ at a specified wavelength λ falls on the radiation-sensitive area of a detector and generates a photocurrent I_{ph}. $s(\lambda)$ is the ratio between the generated photocurrent I_{ph} and the radiation power $\Phi_e(\lambda)$ which falls on the detector.

$$s(\lambda) = \frac{I_{ph}}{\Phi_e(\lambda)}$$

Unit: A/W

$s(\lambda)_{rel}$
Spectral sensitivity, relative
Ratio of the radiant sensitivity $s(\lambda)$ at any considered wavelength to the radiant sensitivity $s(\lambda_o)$ at a certain wavelength λ_o taken as a reference

$$s(\lambda)_{rel} = \frac{s(\lambda)}{s(\lambda_o)}$$

$s(\lambda_o)$
Spectral sensitivity at a reference wavelength λ_o

$s(\lambda_p)$
Spectral sensitivity at a wavelength λ_p

sr
Steradian
Unit of solid angle Ω

T
Period (duration)

T
Temperature
0 K = –273.16°C
Unit: K (Kelvin), °C (Centigrade/degree Celsius)

t
Time

t_{pi}
Input pulse duration

t_{po}
Output pulse duration

T_{amb}
Ambient temperature
If self-heating is significant:
temperature of the surrounding air below the device, under conditions of thermal equilibrium
If self-heating is insignificant:
air temperature in the surroundings of the device

T_{amb}
Ambient temperature range
As an absolute maximum rating:
the maximum permissible ambient temperature range

TK
Temperature coefficient
The ratio of the relative change of an electrical quantity to the change in temperature (ΔT) which causes it under otherwise constant operating conditions

T_{case}
Case temperature
The temperature measured at a specified point on the case of a semiconductor device
Unless otherwise stated, this temperature is given as the temperature of the mounting base for devices with metal can

t_d
Delay time

T_f
color temperature
Temperature of the thermal radiator which emits radiation of the same chromaticity as the radiation considered
Unit: K (Kelvin)

t_f
Fall time

T_j
Junction temperature
The spatial mean value of the temperature during operation. In the case of phototransistors, it is mainly the temperature of the collector junction because its inherent temperature is maximum.

t_{off}
Turn-off time

t_{on}
Turn-on time

t_p
Pulse duration

t_r
Rise time

t_s
Storage time

T_{sd}
Soldering temperature
Maximum allowable temperature for soldering with a specified distance from the case and its duration

T_{stg}
Storage temperature range
The temperature range at which the device may be stored or transported without any applied voltage

V_{BEO}
Base-emitter voltage, open collector

$V_{(BR)}$
Breakdown voltage
Reverse voltage at which a small increase in voltage results in a sharp rise of reverse current. It is given in technical data sheets for a specified current.

$V_{(BR)CEO}$
Collector-emitter breakdown voltage, open base

$V_{(BR)EBO}$
Emitter-base breakdown voltage, open collector

$V_{(BR)ECO}$
Emitter-collector breakdown voltage, open base

V_{CBO}
Collector-base voltage, open emitter
Generally, reverse biasing is carried out by applying a voltage to any of two terminals of a transistor in such a way that one of the junctions operates in reverse direction, whereas the third terminal (second junction) is specified separately.

V_{CE}
Collector-emitter voltage

V_{CEO}
Collector-emitter voltage, open base ($I_B = 0$)

V_{CEsat}
Collector-emitter saturation voltage
The saturation voltage is the dc voltage between collector and emitter for specified (saturation) conditions, i.e., I_C and E_V (E_e or I_B), whereas the operating point is within the saturation region.

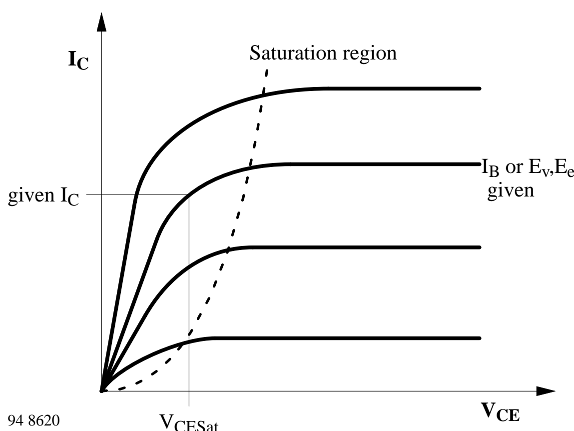

Figure 1.

V_{EBO}
Emitter-base voltage, open collector

V_{ECO}
Emitter-collector voltage, open base

V_F
Forward voltage
The voltage across the diode terminals which results from the flow of current in the forward direction

V_{OC}
Open circuit voltage
The voltage measured between the photovoltaic cell or photodiode terminals at a specified radiation/illumination if the circuit is open

V_{OH}
Output voltage high

V_{OL}
Output voltage low

V_{ph}
Photovoltage
The voltage generated between the photovoltaic cell or photodiode terminals due to radiation/illumination

V_O
Output voltage

V_{no}
Signal-to-noise ratio

V_R
Reverse voltage
The voltage drop which results from the flow of a reverse current

V_S
Supply voltage

$V(\lambda)$
Standard luminous efficiency function for photopic vision (relative human eye sensitivity)

$\varphi = \alpha/_2$
Angle of half sensitivity, angle of half intensity

$\varphi_{1/2}$
Angle of half transmission distance

λ
Wavelength, general
The wavelength of electromagnetic radiation

$\lambda_{0.5}$
Range of spectral bandwidth (50%)
The range of wavelengths where the spectral sensitivity or spectral emission remains within 50% of the maximum value

λ_D
Dominant wavelength

λ_p
Wavelength of peak sensitivity or emission

ΔV_o
Output voltage change (differential output voltage)

$\Delta\lambda$
Spectral half bandwidth
The wavelength interval within which the spectral sensitivity or spectral emission falls to half peak value

Φ_e
Radiant flux, radiant power
Power emitted, transferred, or received in the form of radiation

$$\Phi_e = \frac{dQ_e}{dt}$$

Unit: W (Watt)

Φ_v
Luminous flux
A quantity derived from the radiant flux by spectrally $V(\lambda)$-weighting of the radiation spectrum multiplied by the photometric efficiency constant K_m = 683 lm/W:

$$\Phi_v = K_m \int V(\lambda)\Phi_e(\lambda)d\lambda$$

$$\Phi_v = \frac{dQ_v}{dt}$$

Unit: lm (lumen)

η
Quantum Efficiency

Ω
Solid angle, see figure 2
The space enclosed by rays which emerge from a single point and lead to all the points of a closed curve. If it is assumed that the apex of the cone formed in this way is the center of a sphere with radius r and that the cone intersects with the surface of the sphere, then the size of the surface area (A) of the sphere subtending the cone is a measure of the solid angle

$$\Omega = \frac{A}{r^2}$$

There are 4π sr in a complete sphere. A cone with an angle of half sensitivity $\alpha/2$ forms a solid angle of

$$\Omega = 2\pi\,(1 - \cos\alpha/2) = 4\pi\,\sin^2\alpha/4$$

Unit: sr (Steradian)

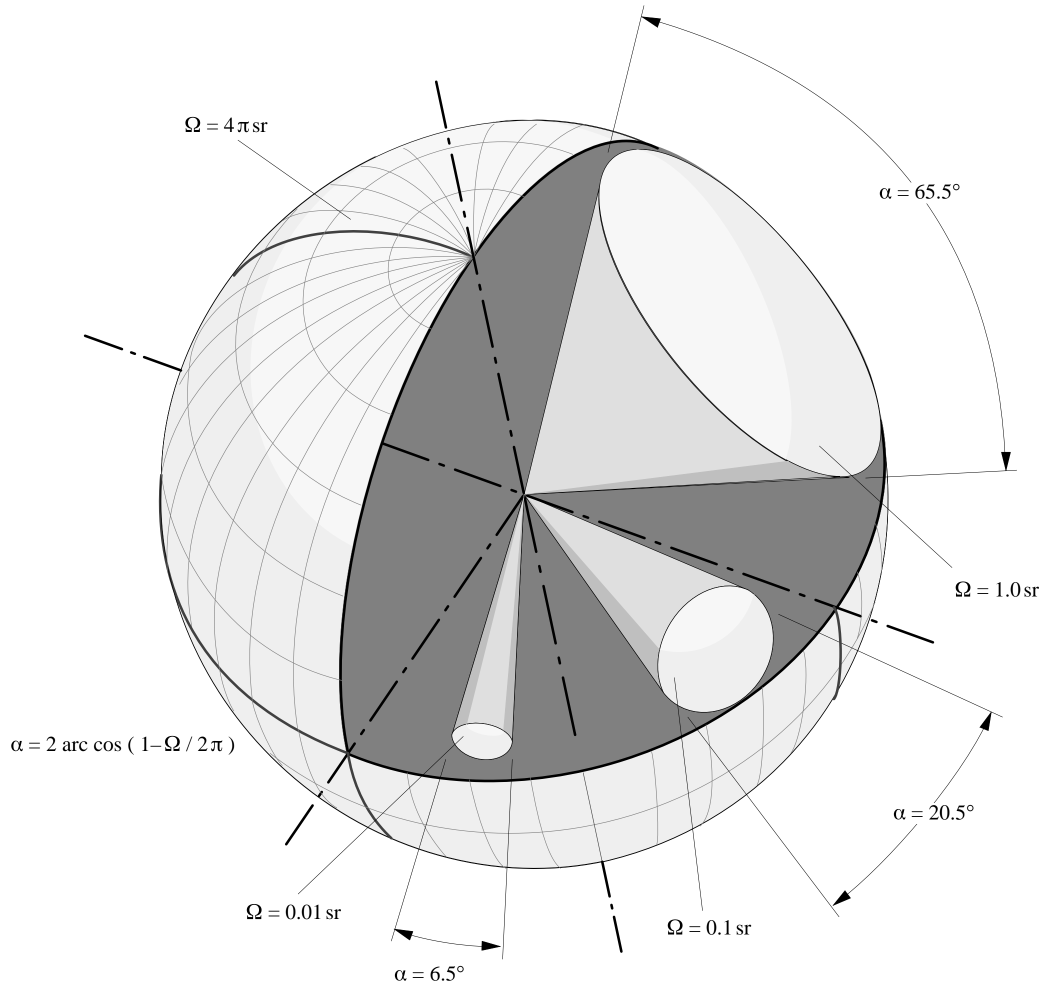

Figure 2.

Examples for Using Symbols According to DIN 41 785 and IEC 148

a) Transistor

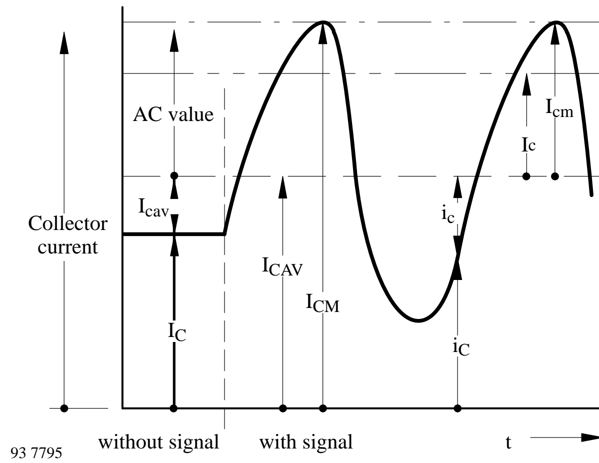

Figure 3.

I_C	dc value, no signal
I_{CAV}	Average total value
I_{CM};I_C	Maximum total value
I_{CEFF}	RMS total value
I_C;I_{CEFF}	RMS varying component
I_{CM};I_C	Maximum varying component value
i_C	Instantaneous total value
i_C	Instantaneous varying component value

It is valid:

$I_{CM} = I_{CAV} + I_{cm}$

$I_{CEFF} = \sqrt{I^2_{CAV} + I^2_{ceff}}$

$i_C = I_{CAV} + i_c$

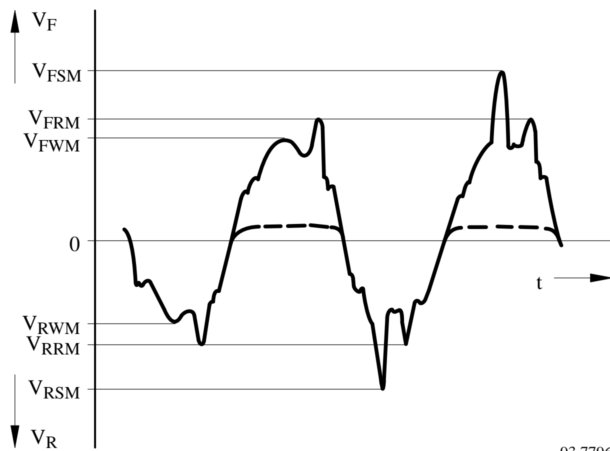

Figure 4.

V_F	Forward voltage
V_R	Reverse voltage
V_{FSM}	Surge forward voltage (non-repetitive)
V_{RSM}	Surge reverse voltage (non-repetitive)
V_{FRM}	Repetitive peak forward voltage
V_{RRM}	Repetitive peak reverse voltage
V_{FWM}	Crest working forward voltage
V_{RWM}	Crest working reverse voltage

c) Designation and symbols of optoelectronic devices are given so far as possible, according to DIN 44020 sheet 1 and IEC publication 50(45).

Table 1. **Terms of Radiometry and Photometry**

Radiometric Units			Photometric Units			
Unit	Symbol	Unit	Unit	Symbol	Unit	Note
Radiant flux, Radiant power	Φ_e	Watt, W	Luminous flux	Φ_v	Lumen, lm	Power
Radiant exitance, Emittance	M_e	W/m^2	Luminous emittance	M_v	lm/m^2	Output power per unit area
(Radiant) intensity	I_e	W/sr	(Luminous) intensity	I_v	Candela, cd, lm/sr	Output power per unit solid angle
Radiant sterance, Radiance	L_e	$\frac{W}{sr\ m^2}$	Luminance (Brightness, sterance)	L_v	cd/m^2	Output power per unit solid angle and emitting area
Radiant incidance, Irradiance	E_e	W/m^2	Illuminance	E_v	lm/m^2 Lux, lx	Input power per unit area
Radiant energy	Q_e	Ws	Luminous energy	Q_v	lm s	Power × time
Irradiation	H_e	Ws/m^2	Illumination	H_v	$lm\ s/m^2$	Radiant energy or luminous energy per unit area

Data Sheet Structure

Data sheet information is generally presented in the following sequence:

- Device description
- Absolute maximum ratings
- Thermal data – Thermal resistances
- Optical and electrical characteristics
- Diagrams
- Dimensions (Mechanical data)

Description, Features, Applications

The following information is provided: Type number, semiconductor materials used, sequence of zones, technology used, device type and, if necessary, construction.

Also, short-form information on special features and typical applications is given.

Absolute Maximum Ratings

These define maximum permissible, operational, and environmental conditions. If any one of these conditions is exceeded, it could result in the destruction of the device.

Unless otherwise specified, an ambient temperature of $25 \pm 3°C$ is assumed for all absolute maximum ratings.

Most absolute ratings are static characteristics; if measured by a pulse method, the associated measurement conditions are stated. Maximum ratings are absolute (i. e., not interdependent).

Any equipment incorporating semiconductor devices must be designed so that even under the most unfavorable operating conditions, the specified maximum ratings of the devices used are never exceeded. These ratings could be exceeded because of changes in

- supply voltage, the properties of other components used in the equipment
- control settings
- load conditions
- drive level
- environmental conditions and the properties of the devices themselves (i.e. ageing).

Thermal Data – Thermal Resistances

Some thermal data (e.g., junction temperature, storage temperature range, total power dissipation) are given under the heading “Absolute maximum ratings”, because they impose a limit on the application range of the device.

The thermal resistance junction ambient (R_{thJA}) quoted is that which would be measured without artificial cooling, i.e., under worst case conditions.

Temperature coefficients are listed together with the associated parameters under “Basic Characteristics” or ”Type Dedicated characteristics”.

Basic Characteristics
Type Dedicated Characteristics

Under these headings, optical, electrical and switching characteristics (minimum, typical and maximum values) are listed as the most important operational characteristics. The associated test conditions, supplemented with curves are also given. An AQL-value is quoted for particularly important parameters.

Diagrams

Besides the static (dc) and dynamic (ac) characteristics, a family of curves is given for specified operating conditions. These curves show the typical interdependence of individual characteristics.

Dimensions (Mechanical Data)

In this section, important dimensions and connection sequences are given, supplemented by a circuit diagram. Case outline drawings carry DIN-, JEDEC or commercial designations. Information on angle of sensitivity or intensity and weight completes the list of mechanical data.

Please note:

If the dimensional information does not include any tolerances, the following applies:

Lead length and mounting hole dimensions are minimum values. Radiant sensitive area (or emitting area respectively) is a typical, all other dimensions are maximum values.

Any device accessories must be ordered separately and the order number must be quoted.

Additional Information

Preliminary specifications

This heading indicates that some information on the device concerned may be subject to slight changes.

Not for new developments

This heading indicates that the device concerned should not be used in equipment under development. It is, however, available for present production.

Physics and Technology

Emitters

Materials

Infrared emitting diodes (IREDs) can be produced from a range of different III-V compounds. Unlike the elemental semiconductor silicon, the compound III-V semiconductors consists of two different elements of group three (e.g., Al, Ga, In) and five (e.g., P, As) of the periodic table. The bandgap energies of these compounds vary between 0.18 eV and 3.4 eV. However, the IREDs considered here emit in the near infrared spectral range between 800 nm and 1000 nm, and, therefore, the selection of materials is limited to GaAs and the mixed crystal $Ga_{1-X}Al_XAs$, $0 \le X < 0.8$, made from the pure compounds GaAs and AlAs.

Infrared radiation is produced by radiative recombination of electrons and holes from the conduction and valence bands. The emitted photon energy, therefore, corresponds closely to the bandgap energy E_g. The emission wavelength can be calculated according to the formula $\lambda(\mu m) = 1.240 / E_g(eV)$. The internal efficiency depends on the band structure, the doping material and the doping level. Direct bandgap materials offer high efficiencies, because no photons are needed for recombination of electrons and holes. GaAs is a direct gap material and $Ga_{1-X}Al_XAs$ is direct up to X = 0.44. The doping species Si provides the best efficiencies and shifts the emission wavelength below the bandgap energy into the infrared spectral range by about 50 nm typically.

Charge carriers are injected into the material via pn junctions. Junctions of high injection efficiency are readily formed in GaAs and $Ga_{1-X}Al_XAs$. P-type conductivity can be obtained with metals of valency two, such as Zn and Mg, n-type conductivity with elements of valency six, such as S, Se and Te. However, silicon of valency four can occupy sites of III-valence and V-valence atoms, and, therefore, acts as donor and as acceptor. The conductivity type depends primarily on the material growth temperature. By employing exact temperature control, pn junctions can be grown with the same doping species Si on both sides of the junction. Ge, on the other hand, also has a valency of four, but occupies group V sites at high temperatures i.e., p-type.

Only monocrystalline material is used for IRED production. In the mixed crystal system $Ga_{1-X}Al_XAs$, $0 \le X < 0.8$, the lattice constant varies only by about 1.5×10^{-3}. Therefore, monocrystalline layered structures of different $Ga_{1-X}Al_XAs$ compositions can be produced with extremely high structural quality. These structures are useful because the bandgap can be shifted from 1.40 eV (GaAs) to values beyond 2.1 eV which enables transparent windows and heterogeneous structures to be fabricated. Transparent windows are another suitable means to increase efficiency, and heterogeneous structures can provide shorter switching times and higher efficiency. Such structures are termed double heterostructures (DH) and consist normally of two layers that confine a layer with a much smaller bandgap.

The best production method for all materials needed is liquid phase epitaxy (LPE). This method uses Ga-solutions containing As, possibly Al, and the doping substance. The solution is saturated at high temperature, typically 900°C, and GaAs substrates are dipped into the liquid. The solubility of As and Al decreases with decreasing temperature. In this way epitaxial layers can be grown by slow cooling of the solution. Several layers differing in composition may be obtained using different solutions one after another, as needed e.g. for DHs.

In liquid phase epitaxial reactors, production quantities of up to 50 wafers, depending on the type of structure required, can be handled .

IRED Chips and Characteristics

At present, the most popular IRED chip is made only from GaAs. The structure of the chip is displayed in figure 5.

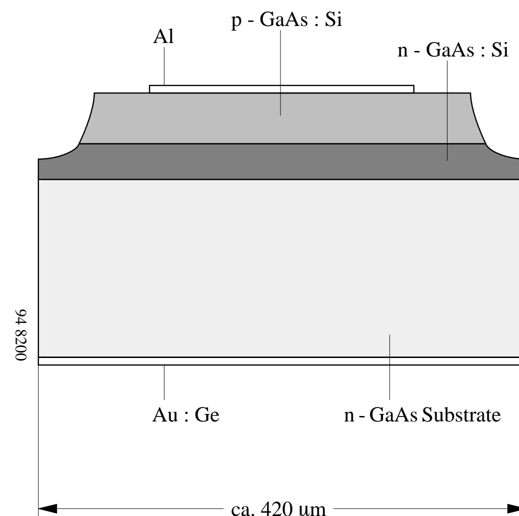

Figure 5.

On an n-type substrate, two Si-doped layers are grown by liquid phase epitaxy from the same solution. Growth starts as n-type at high temperature and becomes p-type below about 820°C. A structured Al-contact on the p-side and a large area Au:Ge contact on the back side provide a very low series resistance. The angular distribution of the emitted radiation is displayed in figure 6.

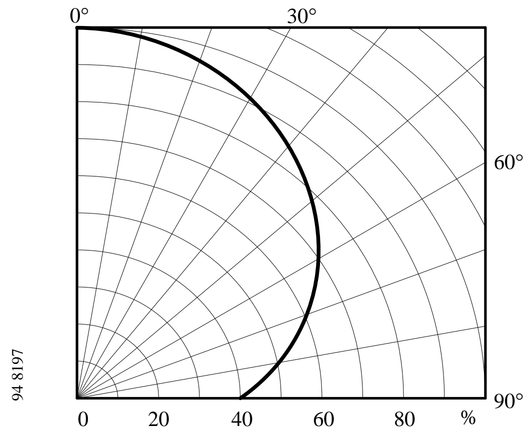

Figure 6.

The package of the chip has to provide good collection efficiency of the radiation emitted sideways, and has to diminish the refractive index step between the chip (n = 3.6) and the air (n = 1.0) with an epoxy of refractive index 1.55. In this way, the output power of the chip is increased by a factor of 3.5 for the assembled device.

The chip described is the most cost-efficient chip. The forward voltage at I_F = 1.5 A has the lowest possible value. The total series resistance is typically only 0.60 Ω. The output power and the linearity (defined as the optical output power increase, divided by the current increase between 0.1 and 1.5 A) are high. Relevant data on the chip and a typical assembled device are given in table 2.

The technology used for another chip eliminates the absorbing substrate and uses only a thick epitaxial layer. The chip is shown in figure 7.

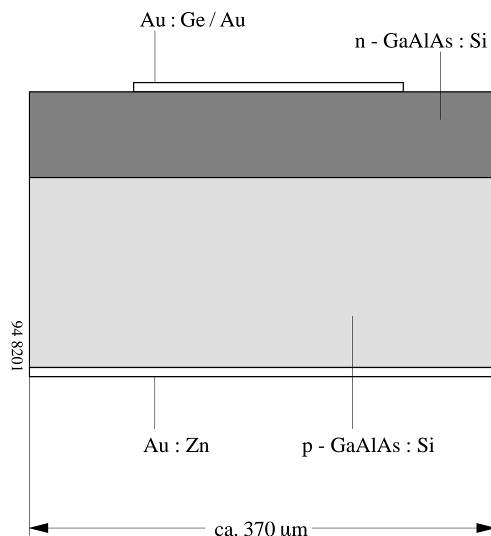

Figure 7.

Originally, the GaAs substrate was adjacent to the n-side. Growth of $Ga_{0.7}Al_{0.3}As$ started as n-type and became p-type – as in the first case – through the specific properties of the doping material Si. A characteristic feature of the Ga-Al-As phase system causes the Al-content of the growing epitaxial layer to decrease. This causes the Al-concentration at the junction to drop to 8% ($Ga_{0.92}Al_{0.08}As$), producing an emission wavelength of 880 nm. During further growth the Al-content approaches zero. The gradient of the Al-content and the correlated gradient of the bandgap energy, produces an emission band of a relatively large half width. The transparency of the large bandgap material results in a very high external efficiency on this type of chip.

The chip is mounted n-side up, and the front side metallization is Au:Ge/Au, whereas the reverse side metallization is Au:Zn.

The angular distribution of the emitted radiation is displayed in figure 8.

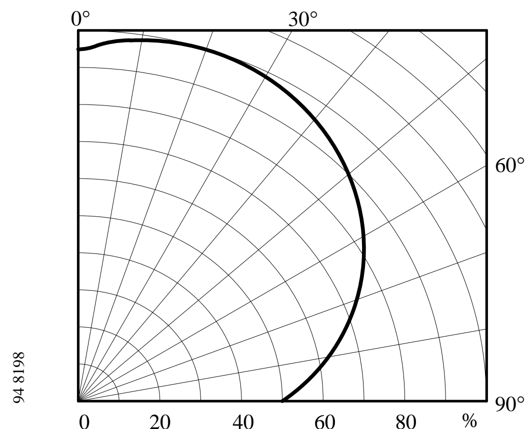

Figure 8.

The $Ga_{1-X}Al_XAs$ chip described has one of the highest output powers of any chip available. Due to its shorter wavelength, the chip offers specific advantages in combination with a Si detector. Integrated Opto-ICs, like amplifiers or Schmitt Triggers, have higher sensitivities at shorter wavelengths. Similarly, phototransistors are also more sensitive. Finally, the frequency bandwidth of pin diodes is higher at shorter wavelengths. This chip also has the advantage of having high linearity up to and beyond 1.5 A. The forward voltage, however, is higher than the voltage of a GaAs chip. Table 2 provides more data on the chip.

A technology combining some of the advantages of the two technologies described above is summarized in figure 9.

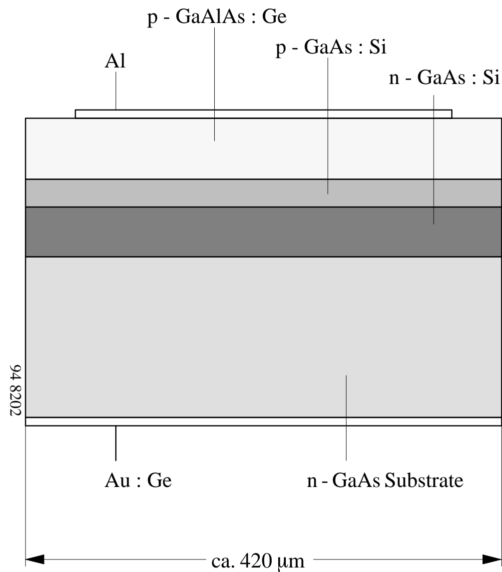

Figure 9.

Starting with the n-type substrate, n- and p-type GaAs layers are grown in a similar way to the epitaxy of the standard GaAs:Si diode. After this, a highly transparent window layer of $Ga_{1-X}Al_XAs$, doped p-type with Ge, is grown. The upper contact to the p-side is made of Al and the rear side contact is Au:Ge. The angular distribution of the emitted radiation is shown in figure 10.

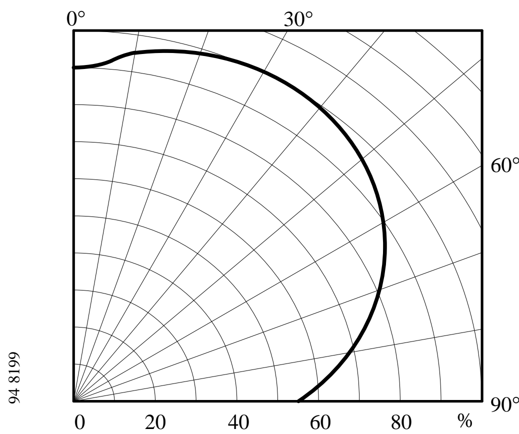

Figure 10.

This chip type combines a relatively low forward voltage with a high electro-optical efficiency, offering optimized combination between the advantageous characteristics of the two other chips. Refer again to table 2 for more details.

As mentioned in the previous section, double heterostructures (DH) provide even higher efficiencies and faster switching times. A schematical representation of such a chip is shown in figure 11.

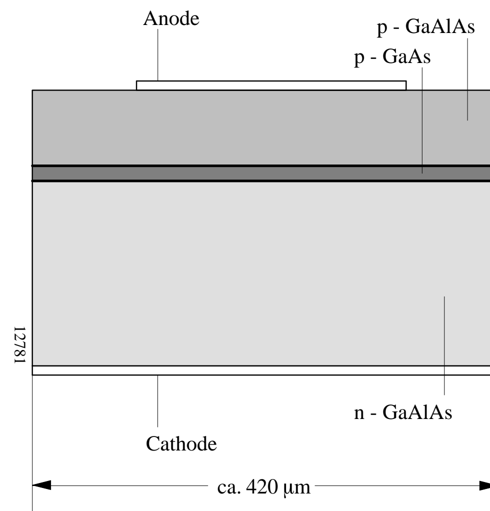

Figure 11.

The active layer is depicted as the thin layer between the p- and n-type $Ga_{1-X}Al_XAs$ confinement layers. The contacts are dependent on the polarity of the chip. If p is up, then the p-side contact is Al, the back side Au:Ge, and if n is up, then this side has a Au:Ge contact and the back side Au:Zn.
Two such chips that are also very suitable for IrDA applications are given in table 2.

Table 2. Characteristic data of IRED chips

Technology	Typical Chip Data				Typical Device	Typical Device Data				
	Φe/mW at 0.1 A	λp/nm	Δλ/nm	Polarity		Φe/mW at 0.1 A	Φe/mW at 1.5 A	V_F/V at 0.1 A	V_F/V at 1.5 A	Φe(1.5A)/ Φe(0.1A)
GaAs on GaAs	4.3	950	50	p up	TSUS 540.	15	140	1.3	2.1	9
$Ga_{1-X}Al_XAs$	6.7	875	80	n up	TSHA 550.	27	350	1.5	3.4	13
GaAs + $Ga_{1-X}Al_XAs$ on GaAs	5.8	925	50	p up	TSIP 520.	24	300	1.3	2.4	12
$Ga_{1-X}Al_XAs$ on $Ga_{1-X}Al_XAs$	11	870	40	p up	TSHF 540.	32		1.3		t_r,t_f /ns 30
$Ga_{1-X}Al_XAs$ on $Ga_{1-X}Al_XAs$	16	870	40	n up	TSPF 5400	40		1.5		30

UV, Visible, and Near IR Silicon Photodetectors

(adapted from ”Sensors, Vol 6, Optical Sensors, Chapt. 8, VCH – Verlag, Weinheim 1991)

Silicon Photodiodes

The physics of silicon detector diodes

The absorption of radiation is caused by the interaction of photons and the charge carriers inside a material. The different energy levels allowed and the band structure determine the likelihood of interaction and, therefore, the absorption characteristics of the semiconductors. The long wavelength cutoff of the absorption is given by the bandgap energy. The slope of the absorption curve depends on the physics of the interaction and is much weaker for silicon than for most other semiconducting materials. This results in the strong wavelength-dependent penetration depth which is shown in figure 12. (The penetration depth is defined as that depth where 1/e of the incident radiation is absorbed.)

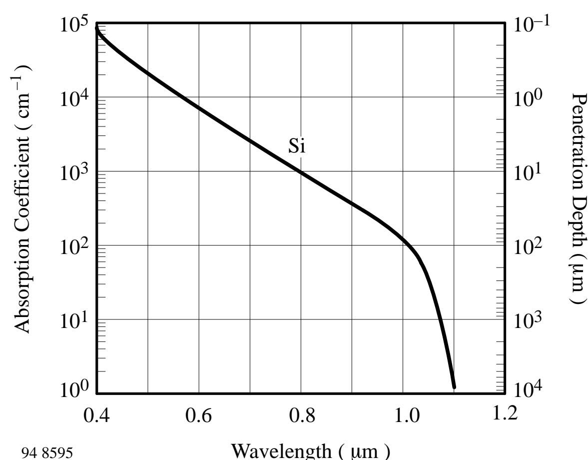

Figure 12. Absorption and penetration depth of optical radiation in silicon

Depending on the wavelength, the penetration depth varies from tenths of a micron at 400 nm (blue) to more than 100 µm at 1 µm (IR). For detectors to be effective, an interaction length of at least twice the penetration depth should be realized (equivalent to $1/e^2 = 86\%$ absorbed radiation). In the pn diode, the generated carriers are collected by the electrical field of the pn junction. The effects in the vicinity of a pn junction are shown in figure 13 for

various types and operating modes of the pn diode. The incident radiation generates mobile minority carriers – electrons in the p-side, holes in the n-side. In the short circuit mode shown in figure 13 (top), the carriers drift under the field of the built-in potential of the pn junction. Other carriers diffuse inside the field-free semiconductor along a concentration gradient, which results in an electrical current through the applied load, or without load, in an external voltage, the open circuit voltage, V_{OC}, at the contact terminals. The bending of the energy bands near the surface is caused by surface states. An equilibrium is established between the generation, the recombination of carriers, and the current flow through the load.

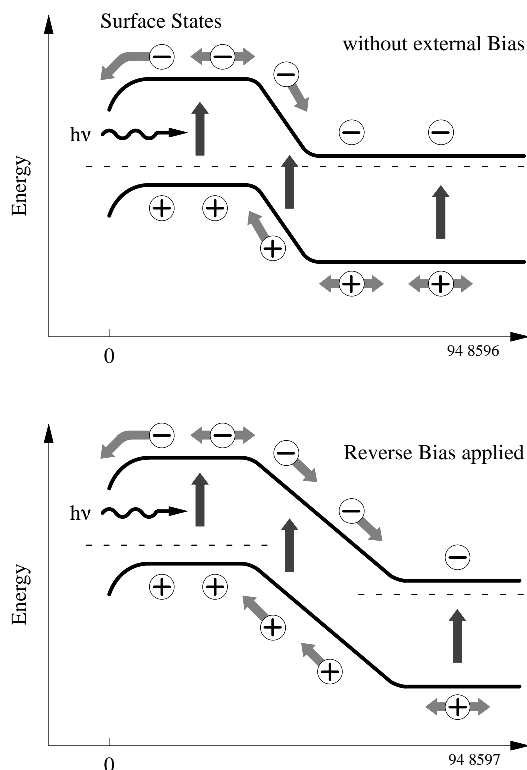

Figure 13. Generation-recombination effects in the vicinity of a pn junction. Top: Short circuit mode, bottom: reverse biased

The recombination takes place inside the bulk material with technology- and process-dependent time constants which are very small near the contacts and the surfaces of the device. For short wavelengths with very small penetration depths, the carrier recombination is the efficiency limiting process. To achieve high efficiencies, as many carriers as possible should be separated by the electrical field inside the space charge region. This is a very fast process, much faster than the typical recombination times (for data, see chapter 'Operating modes and circuits'). The width, W, of the space charge is a function of the doping concentration N_B and the applied voltage V:

$$W = \sqrt{\frac{2 \times \epsilon_s \times (V_{bi} + V)}{q \times N_B}} \qquad (1.1)$$

(for a one-sided abrupt junction), where V_{bi} is the built-in voltage, ε_s the dielectric constant of Si, and q the electronic charge. The diode's capacitance (which can be speed limiting) is also a function of space charge width and applied voltage. It is given by

$$C = \frac{\epsilon_s \times A}{W} \qquad (1.2)$$

where A is the area of the diode. An externally applied bias will increase the space charge width (see figure 13) with the result that a larger number of carriers are generated inside this zone which can be flushed out very fast with high efficiency under the applied field. From equation 1.1, it is evident that the space charge width is a function of the doping concentration N_B. Diodes with a so-called pin structure show a wide space charge width where i stands for intrinsic, very low doped. This zone is also sometimes nominated as ν or p rather than low doped n, n^- or p, p^-zone indicating the very low doping.

In figure 14, the different behavior of low doped pin diodes and pn diodes is shown. The space charge width of the pin diode (bottom) with a doping level ($n=N_B$) as low as $N_B = 5 \times 10^{11}$ cm^{-3} is about 80 µm wide for a 2.5 V bias in comparison with a pn diode with a doping (n) of $N_B = 5 \times 10^{15}$ cm^{-3} with only 0.8 µm.

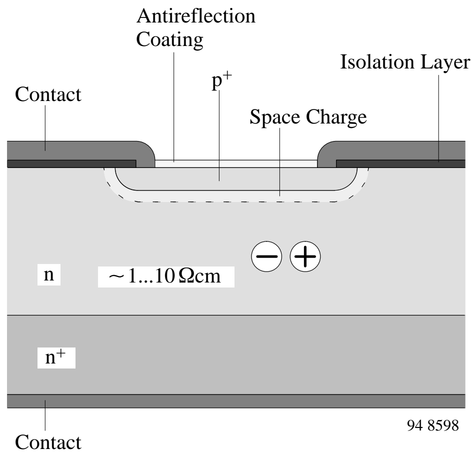

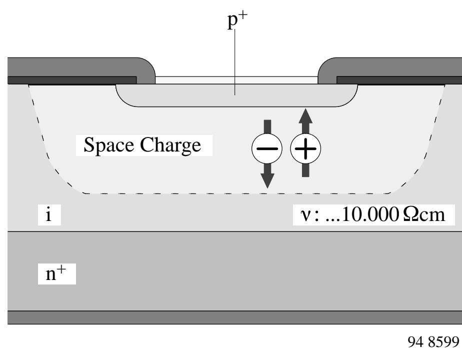

Figure 14. Comparison of pn diode (top) and pin diode (bottom)

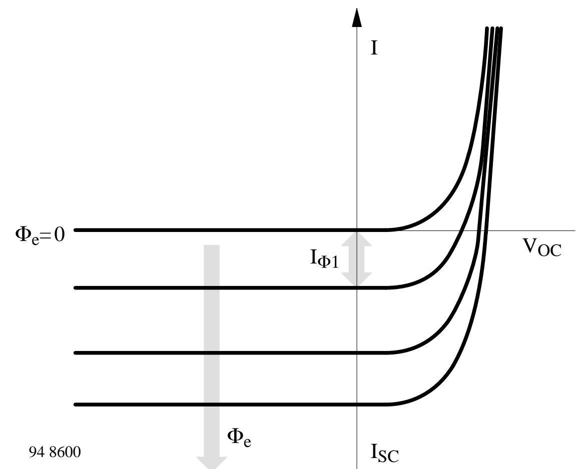

Figure 15. I-V-Characteristics of an Si photodiode under illumination. Parameter: Incident radiant flux

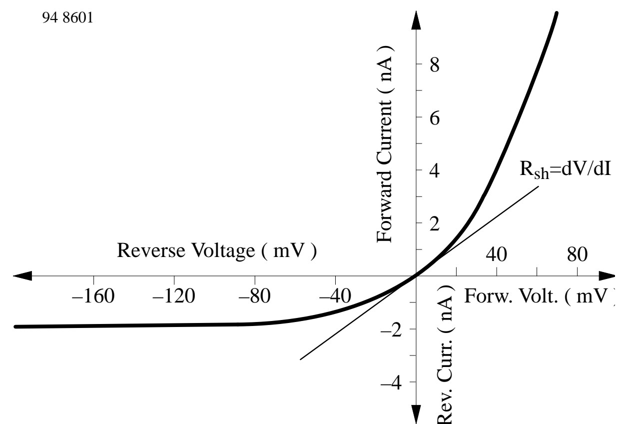

Figure 16. Measured I-V-characteristics of an Si photodiode in the vicinity of the origin

Properties of Silicon Photodiodes

I-V Characteristics of illuminated pn junction

The I-V-characteristics of a photodiode are shown in figure 15. The characteristic of the non illuminated diode is identical to the characteristic of a standard rectifier diode. The relationship between current, I, and voltage, V, is given by

$$I = I_S \times (\exp V/V_T - 1) \qquad (2.1)$$

with $V_T = kT/q$
$k = 1.38 \times 10^{-23}$ JK^{-1}, Boltzmann constant
$q = 1.6 \times 10^{-19}$ As, electronic charge.

I_s, the dark-reverse saturation current, is a material and technology-dependent quantity. The value is influenced by the doping concentrations at the pn junction, by the carrier lifetime, and especially by the temperature. It shows a strongly exponential temperature dependence and doubles every 8°C.

Typical dark currents of Si photodiodes are dependent on size and technology and range from less than picoamps up to tens of nanoamps at room temperature conditions. As noise generators, the dark current I_{r0} and the shunt resistance R_{sh} (defined and measured at a voltage of 10 mV forward or reverse, or peak-to-peak) are limiting quantities when detecting very small signals.

The photodiode exposed to optical radiation generates a photocurrent I_r exactly proportional to the incident radiant power Φ_e. The quotient of both is the spectral responsivity s(λ),

$$s(\lambda) = I_r/\phi_e \; [A/W] \qquad (2.2)$$

The characteristic of the irradiated photodiode is then given by

$$I = I_S \times (\exp V/V_T - 1) - s(\lambda) \times \phi_e \qquad (2.3)$$

and in the case $V \approx 0$, zero or reverse bias we find,

$$I = -I_s - s(\lambda) \times \phi_e$$

Dependent on load resistance, R_L, and applied bias, different operating modes can be distinguished. The unbiased diode operates in the photovoltaic mode. Under short circuit conditions (load $R_L = 0\ \Omega$), the short circuit current, I_{SC} flows into the load. When R_L increases to infinity, the output voltage of the diode rises to the open circuit voltage, V_{OC}, given by

$$V_{OC} = V_T \times \ln(\ s(\lambda) \times \phi_e / I_s + 1) \qquad (2.4)$$

Because of this logarithmic behavior, the open circuit voltage is sometimes used for optical lightmeters in photographic applications. The open circuit voltage shows a strong temperature dependence with a negative temperature coefficient. The reason for this is the exponential temperature coefficient of the dark reverse saturation current I_s. For precise light measurement, a temperature control of the photodiode is employed. Precise linear optical power measurements require small voltages at the load typically smaller than about 5% of the corresponding open circuit voltage. For less precise measurements, an output voltage of half the open circuit voltage can be allowed. The most important disadvantage of operating in the photovoltaic mode is the relative large response time. For faster response, it is necessary to implement an additional voltage source reverse biasing the photodiode. This mode of operation is termed the photoconductive mode. In this mode, the lowest detectable power is limited by the shot noise of the dark current, I_s, while in the photovoltaic mode, the thermal (Johnson) noise of the shunt resistance, R_{sh}, is the limiting quantity.

Spectral responsivity

Efficiency of Si photodiodes:

The spectral responsivity, s_λ, is given as the number of generated charge carriers ($\eta \times N$) per incident photons N of energy $h \times \nu$ (η is the percent efficiency, h is Plancks constant, and ν is the frequency of radiation). Each photon will generate one charge carrier at the most . The photocurrent I_{re} is then given as

$$I_{re} = \eta \times N \times q$$

$$s_\lambda = I_{re}/\phi_e$$

$$= \eta \times N \times q/(h \times \nu \times N) = \eta \times q/(h \times \nu)$$

$$s_\lambda = \frac{\lambda(\mu m)}{1.24}\ [A/W]$$

At fixed efficiency, a linear relationship between wavelength and spectral responsivity is valid.

Figure 12 shows that semiconductors absorb radiation similar to a cut-off filter. At wavelengths smaller than the cut-off wavelength the incident radiation is absorbed. At larger wavelengths the radiation passes through the material without interaction. The cut-off wavelength corresponds to the bandgap of the material. As long as the energy of the photon is larger than the bandgap, carriers can be generated by absorption of photons, provided that the material is thick enough to propagate photon-carrier interaction. Bearing in mind that the energy of photons decreases with increasing wavelength, it can be understood, that the curve of the spectral responsivity vs. wavelength in the ideal case (100% efficiency) will have a triangular shape (see figure 17). For silicon photodetectors, the cut-off wavelength is near 1100 nm.

In most applications, it is not necessary to detect radiation with wavelengths larger than 1000 nm. Therefore, designers use a typical chip thickness of 200 µm to 300 µm, which results in reduced sensitivity at wavelengths larger than 950 nm . With a typical chip thickness of 250 µm, an efficiency of about 35% at 1060 nm is achieved. At shorter wavelengths (blue-near UV, 500 nm to 300 nm) the sensitivity is limited by recombination effects near the surface of the semiconductor. The reduction in the efficiency starts near 500 nm and increases with decreasing wavelength. Standard detectors designed for visible and near IR radiation may have only poor UV/blue sensitivity and poor UV stability. Well designed sensors for wavelengths of 300 to 400 nm can operate with fairly high efficiencies. At smaller wavelengths (< 300 nm), the efficiency decreases strongly.

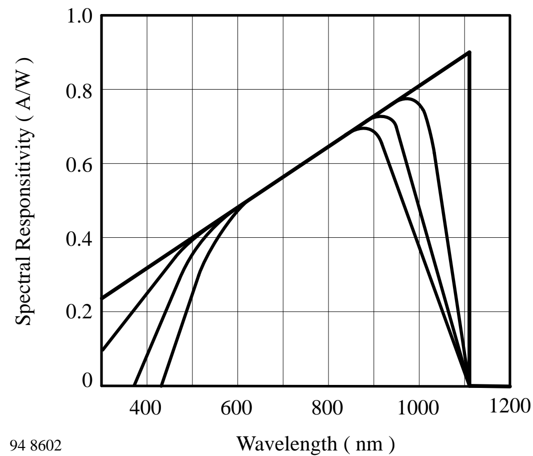

Figure 17. Spectral responsivity as a function of wavelength of a Si photodetector diode, ideal and typical values

Temperature dependence of spectral responsivity

The efficiency of carrier generation by absorption and the loss of carriers by recombination are the factors which influence the spectral responsivity. The absorption

coefficient increases with temperature. Radiation of long wavelength is therefore more efficiently absorbed inside the bulk, and results in increased response. For shorter wavelengths (< 600 nm), reduced efficiency is observed with increasing temperature because of increased recombination rates near the surface. These effects are strongly dependent on technological parameters and therefore cannot be generalized to the behavior at longer wavelengths.

Uniformity of spectral responsivity

Inside the technologically defined active area of photodiodes, the spectral responsivity shows a variation of the sensitivity in the order of < 1%. Outside the defined active area, especially at the lateral edges of the chips, the local spectral response is sensitive to the applied reverse voltage. Additionally, this effect depends on the wavelength. Therefore, the relation between power (Watt) related spectral responsivity, s_λ (A/W), and power density (Watt/cm^2) related spectral responsivity, s_λ [A/(W/cm^2)] is not a constant. This relation is a function of wavelength and reverse bias.

Stability of spectral responsivity

Si detectors for wavelengths between 500 nm and 800 nm appear to be stable over very long periods of time. In the literature concerned here, remarks can be found on instabilities of detectors in the blue, UV, and near IR under certain conditions. Thermal cycling reversed the degradation effects. Surface effects and contamination are possible causes but are technologically well controlled.

Angular dependence of responsivity

The angular response of Si photodiodes is given by the optical laws of reflection. The angular response of a detector is shown in figure 18.

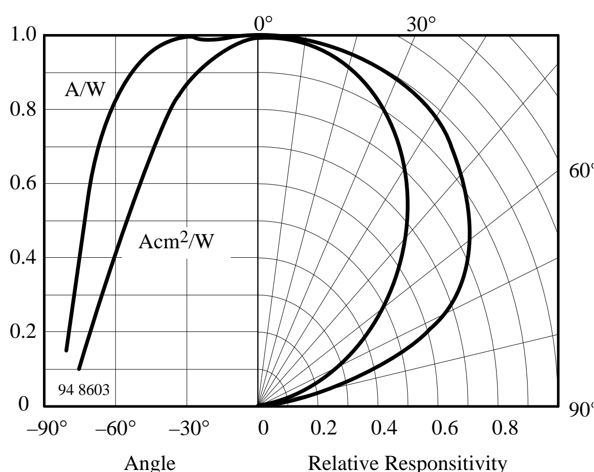

Figure 18. Responsivity of Si photodiodes as a function of the angle of incidence

The semiconductor surfaces are covered with quarter wavelength anti-reflection coatings. The encapsulation is performed with uncoated glass or sapphire windows.

The bare silicon response can be altered by optical imaging devices such as lenses. In this way, nearly every arbitrary angular response can be achieved.

Dynamic Properties of Si Photodiodes

Si photodiodes are available in many different variations. The design of the diodes can be tailored to meet special needs. Si photodiodes may be designed for maximum efficiency at given wavelengths, for very low leakage currents, or for high speed. The design of a photodiode is nearly always a compromise between various aspects of a specification.

Inside the absorbing material of the diode, photons can be absorbed in different regions. For example at the top of a p^+n^{-}-diode there is a highly doped layer of p^+ -Si. Radiation of shorter wavelengths will be effectively absorbed, but for larger wavelengths only a small amount is absorbed. In the vicinity of the pn junction, there is the space charge region, where most of the photons should generate carriers. An electric field accelerates the generated carrier in this part of the detector to a high drift velocity. The carriers which are not absorbed in these regions penetrate into the field-free region where the motion of the generated carriers fluctuates by the slow diffusion process.

The dynamic response of the detector is composed of the different processes which transport the carriers to the contacts. The dynamic response of photodiodes is influenced by three fundamental effects:

- Drift of carriers in an electric field
- Diffusion of carriers
- Capacitance × load resistance

The carrier drift in the space charge region occurs rapidly with very small time constants. Typically, the transit times in an electric field of 0.6 V/µm are in the order of 16 ps/µm and 50 ps/µm for electrons and holes, respectively. At the (maximum) saturation velocity, transit time is in the order of 10 ps/µm for electrons in p-material. With a 10 µm drift region, travelling times of 100 ps can be expected. The response time is a function of the distribution of the generated carriers and is therefore dependent on the wavelength.

The diffusion of carriers is a very slow process. The time constants are in the order of some µs.

The typical pulse response of detectors is dominated by these two processes. Obviously, carriers should be absorbed in large space charge regions with high internal electrical fields. This requires material with an adequate low doping level. Furthermore, a reverse bias of rather large voltage is useful. Radiation of shorter wavelength is absorbed in smaller penetration depths. At wavelengths

shorter than 600 nm, decreasing wavelength leads to an absorption in the diffused top layer. The movement of carriers in this region is also diffusion limited. Because of small carrier lifetimes, the time constants are not as large as in homogeneous substrate material.
Finally, the capacitive loading of the output in combination with the load resistance limits the frequency response.

Properties of Silicon Phototransistors

The phototransistor is equivalent to a photodiode in conjunction with a bipolar transistor amplifier (figure 19). Typically, current amplification, B, is between 100 and 1000 depending on the type and application. The active area of the phototransistor is usually about 0.5×0.5 mm^2. Data of spectral responsivity are equivalent to those of photodiodes, but must be multiplied by the factor of the current amplification, B.

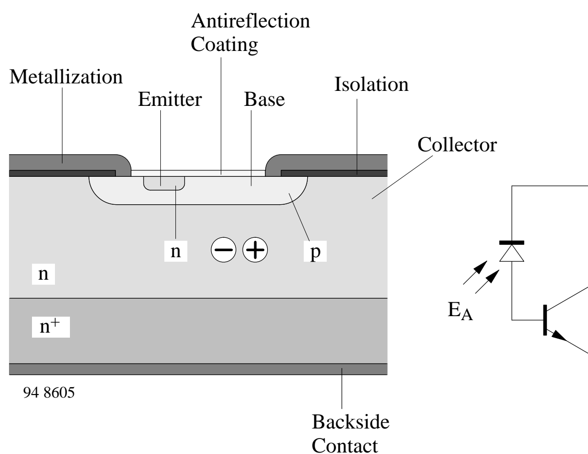

Figure 19. Phototransistor, cross section and equivalent circuit

The switching times of phototransistors are dependent on the current amplification and load resistance and are between 30 µs and 1 µs. The resulting cut-off frequencies are a few hundred kHz.

The transit times, t_r and t_f, are given by

$$t_{r,f} = \sqrt{(1/2f_t^2)^2 + b(RC_BV)^2}$$

f_t: Transit frequency
R: Load resistance
C_B: Base-collector capacitance, b= 4...5
V: Amplification

Phototransistors are most frequently applied in interrupters and opto-isolators.

Applications

Silicon photodetectors are used in manifold applications, such as sensors for radiation from the near UV over the visible to the near infrared. There are numerous applications in the measurement of light, such as dosimetry in the UV, photometry, and radiometry. A well known application is shutter control in cameras.

Another large application area for detector diodes and especially phototransistors, is that of position sensing. Examples are quadrant detectors, differential diodes, interruptors, and reflex sensors.

Other types of silicon detectors are built-in as parts of optocouplers, or optoisolators.

One of the largest application areas is the remote control of TV sets and other home entertainment appliances.

Different applications require specialized detectors and also special circuits to enable optimized functioning.

Equivalent circuit

Photodetector diodes can be described by the electrical equivalent circuit shown in figure 20.

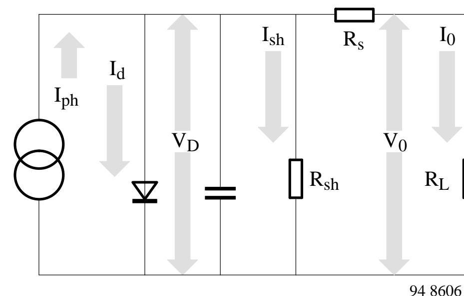

Figure 20.

$$I_O = I_{ph} - I_D - I_{sh}$$

$$I_O = I_{ph} - I_s(\exp\frac{qV_D}{kT} - 1) - I_{sh}$$

$$V_{OC} = V_T \times \ln\left(\frac{s(\lambda) \times \phi_e - I_{sh}}{I_s} + 1\right)$$

As described in chapter 'I-V Characteristics of illuminated pn junction', the incident radiation generates a photocurrent loaded by a diode characteristic and the load resistor, R_L. The other parts of the equivalent circuit (the parallel capacitance, C, combined from junction, C_j, and stray capacitances, the serial resistance, R_S, and the shunt resistance, R_{sh}, representing an additional leakage) can be neglected in most of the standard applications, and are not expressed in equations 2.3 and 2.4. However, in applications with high frequencies or extreme irradiation levels, these parts must be regarded as limiting elements.

Searching for the right detector diode type

The photodiode BPW 20 R is a pn diode based on rather highly doped n-silicon, while the S153P is a pin diode

based on very lightly doped n-silicon. Both diodes have the same active area and the spectral response as a function of the wavelength is very similar. The diodes differ in the junction capacitance and shunt resistance both of which can influence the performance in the application.

Detecting very small signals is the domain of the pn diodes with their very small dark currents and dark/shunt resistances. With a specialized detector technology, these parameters are very well controlled in all TEMIC photodetectors.

The very small leakage currents of pn diodes are offset by higher capacitances and smaller bandwidths in comparison to pin diodes.

Photodiodes are often operated in the photovoltaic mode (especially in light meters) , as depicted in the circuit of figure 21, where a strong logarithmic dependence of the open circuit voltage on the input signal is used.

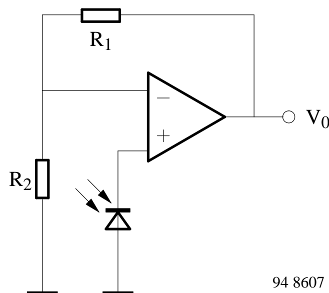

$$V_O \approx V_{OC} \times [1 + R_1/R_2] \quad \text{with}$$

$$V_{OC} = V_T \times \ln(s(\lambda) \times \phi_e/I_s + 1)$$

Figure 21. Photodiode in the photovoltaic mode operating with a voltage amplifier

It should be noted that the extremely high shunt/dark resistance (more than 15 GΩ) combined with a high-impedance operational amplifier input and a junction capacitance of about 1 nF can result in slow switch-off time constants of some seconds. Some instruments therefore have a reset button for shortening the diode before starting a measurement. The photovoltaic mode of operation for precise measurements should be limited to the range of low ambient temperatures, or a temperature control of the diode (e.g., using a Peltier cooler) should be applied. At elevated temperatures, the dark current is increased (see figure 22) leading to a non-logarithmic and temperature dependent output characteristic (see figure 23). The curves shown in figure 22 represent the typical behavior of these diodes. The guaranteed leakage (dark reverse current) is specified with I_{ro} = 30 nA for the standard types. This value is far from the one which is typically measured. Tighter customer specifications are available on request. The curves of figure 23 show the open circuit voltage as a function of the irradiance with the dark reverse current, I_S, as parameter (in a first approximation increasing I_S and I_{sh} have the same effect). The parameter covers the possible spread of dark current. In combination with figure 22 one can project the extreme dependence of the open circuit voltage at high temperatures (figure 24).

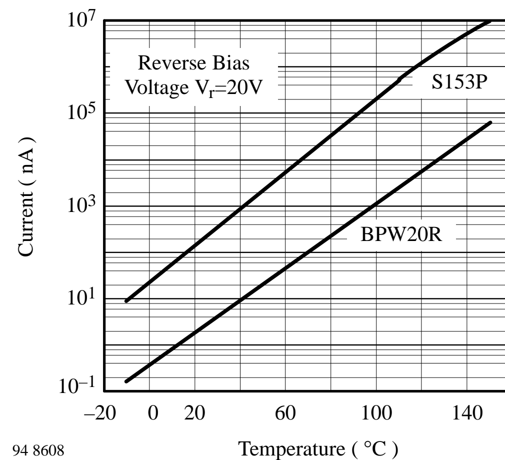

Figure 22. Dark reverse current vs. temperature

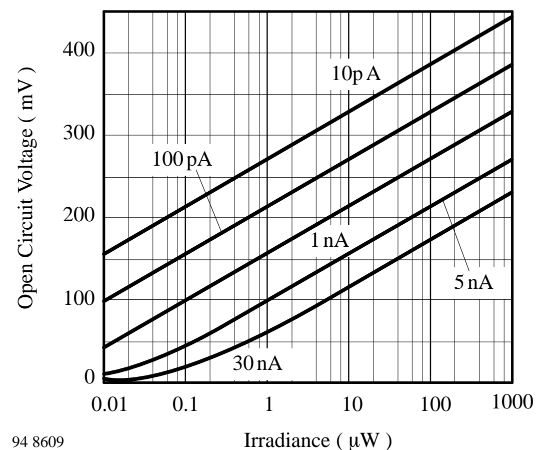

Figure 23. Open circuit voltage vs. irridiance, parameter: dark reverse current, BPW 20 R

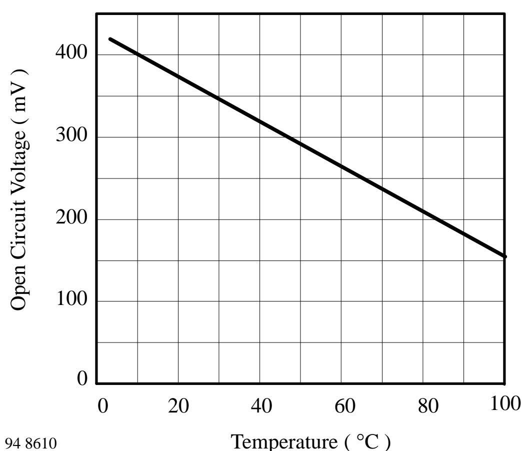

Figure 24. Open circuit voltage vs. temperature, BPW46

Operating modes and circuits

The advantages and disadvantages of operating a photodiode in the open circuit mode have been discussed.

For operation in the short circuit (see figure 25) or photoconductive (see figure 26) mode, current-to-voltage converters are typically used. In comparison with the photovoltaic mode, the temperature dependence of the output signal is much lower. Generally the temperature coefficient of the light reverse current is positive for irradiation with wavelengths > 900 nm, rising with increasing wavelength. For wavelengths < 600 nm, a negative temperature coefficient is found, likewise with increasing absolute value to shorter wavelengths. Between these wavelength boundaries the output is almost independent of temperature. By using this mode of operation, reverse biased or unbiased (short circuit conditions), the output voltage, Vo, will be directly proportional to the incident radiation, ϕ_e (see the equation in figure 25).

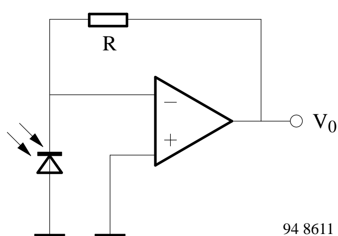

$$V_O = -R \times \Phi_e \times s(\lambda)$$

$$V_O = -I_{SC} \times R$$

Figure 25. Transimpedance amplifier, current to voltage converter, short circuit mode

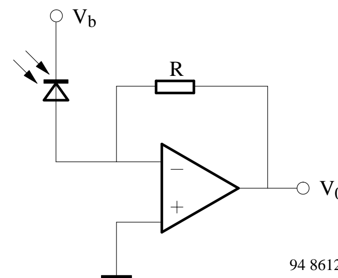

Figure 26. Transimpedance amplifier, current to voltage converter, reverse biased photodiode

The circuit in figure 25 minimizes the effect of the reverse dark current while the circuit in figure 26 improves the speed of the detector diode due to a wider space charge region with decreased junction capacitance and field increased velocity of the charge carrier transport.

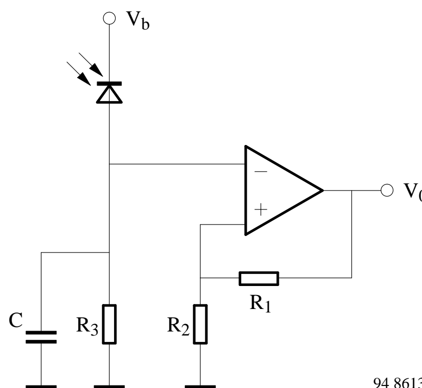

Figure 27. RC-loaded photodiode with voltage amplifier

Figure 27 shows photocurrent flowing into an RC load, where C represents the junction and stray capacitance while R_3 can be a real or complex load, such as a resonant circuit for the operating frequency.

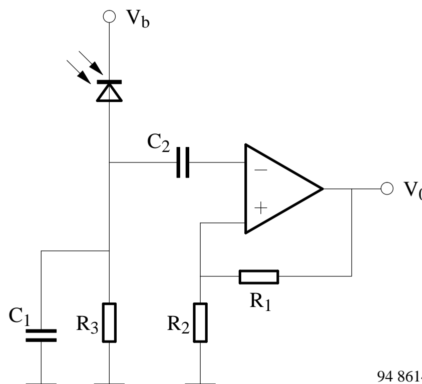

$$V_O \approx \phi_e \times s(\lambda) \times R_3 \times [1 + R_1/R_2]$$

Figure 28. AC-coupled amplifier circuit

The circuit in figure 28 is equivalent to figure 27 with a change to AC coupling. In this case, the influence of the

background illumination can be separated from a modulated signal. The relation between input signal (irradiation, ϕ_e) and output voltage is given by the equation in figure 28.

Frequency response

The limitations of the switching times in pn diodes is determined by the carrier lifetime. Due to the absorption properties of silicon, especially in pn diodes, most of the incident radiation at longer wavelengths is absorbed outside the space charge region. Therefore, a strong wavelength dependence of the switching times can be observed (figure 29).

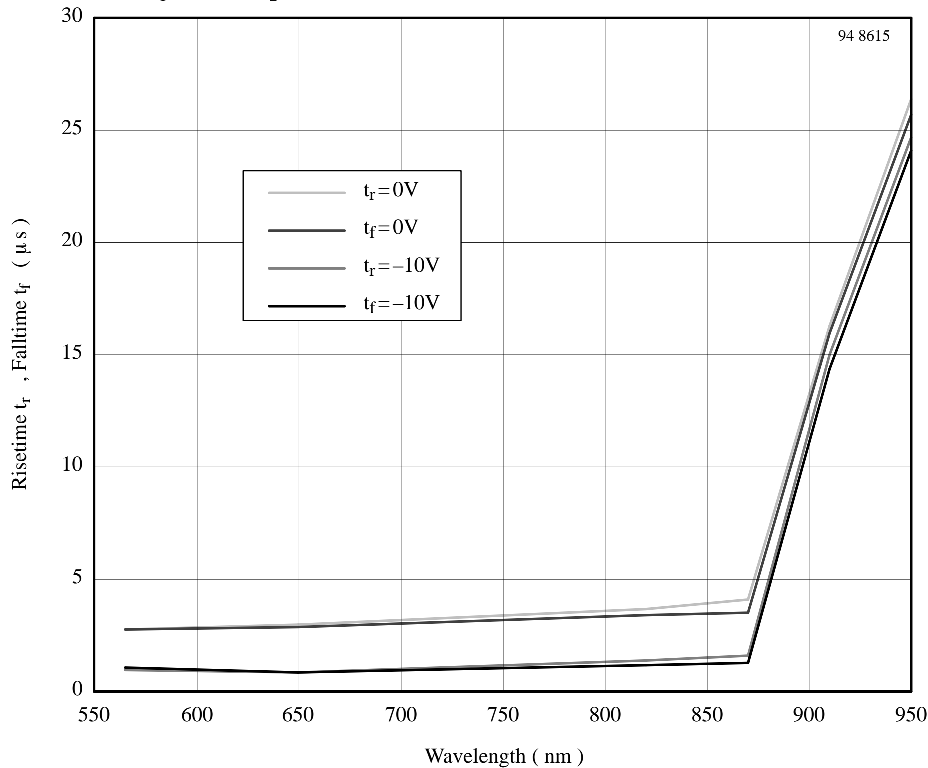

Figure 29. Switching times vs. wavelength for photodiode BPW 20 R

A drastic increase in rise and fall times is observed at wavelengths > 850 nm. The differences between unbiased and biased operation result from the widening of the space charge region.

However, for the pin diodes (BPW34/ S153P family) similar results with shifted time scales are found. This behavior, in this case in the frequency domain, is presented in figure 30 for a wavelength of 820 nm and figure 31. for 950 nm.

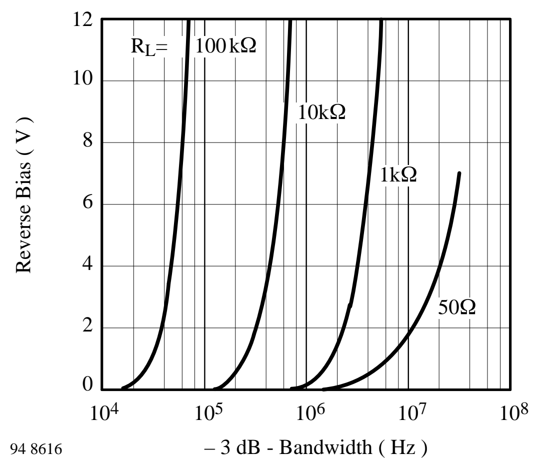

Figure 30. BPW 41-family, bandwidth vs. reverse bias voltage, parameter: load resistance, λ = 820 nm

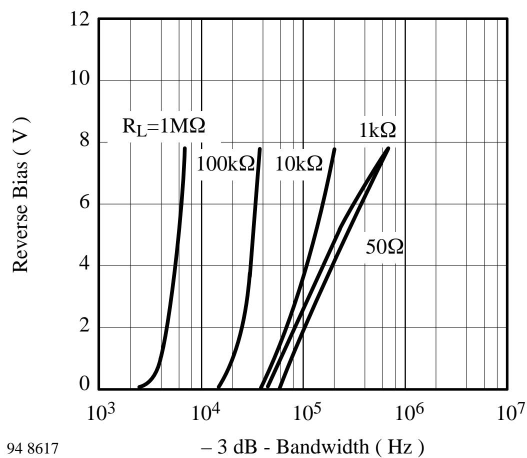

Figure 31. BPW 41-family, bandwidth vs. reverse bias voltage, parameter: load resistance, λ = 950 nm

Below about 870 nm, only slight wavelength dependence can be recognized, while a steep change of cut-off frequency takes place from 870 nm to 950 nm (different time scales in figure 30 and figure 31 !). Additionally, the influence of the load resistances and the reverse bias voltages can be taken from these diagrams.

For cut-off frequencies greater 10–20 MHz, depending on the supply voltage available for biasing the detector diode, pin diodes are also used. However, for this frequency range, and especially when operating with low bias voltages, thin epitaxially grown intrinsic (i) layers are incorporated into the pin diodes. As a result, these diodes (e.g., TEMICs BPW97) can operate with low bias voltages (3 to 4 V) with cut-off frequencies of 300 MHz at a wavelength of 790 nm. With application-specific optimized designs, pin diodes with cutoff frequencies up to 1 GHz at only a 3 V bias voltage with only an insignificant loss of responsivity can be generated.

For operating these fast diodes in combination with current voltage converters, transimpedance amplifiers, signal regenerators and LED drivers are available from TEMIC (Transimpedance amplifier: U6791, regenerator: U6792, and LED driver: U6795).

The main applications for these photodiodes are found in optical local area networks operating in the first optical window at wavelengths of 770 nm to 880 nm.

Which type for which application?

In table 3, selected diode types are assigned to different applications. For more precise selection according to chip sizes and packages, refer to the tables in the introductory pages of this data book.

Table 3. Photo diode reference table

Detector application	pin diode	pn diode	epi-pin diode
Photometry, lightmeter		BPW 21 R	
Radiometry	S 153 P, BPW 34, ...	BPW 20 R	
Light barriers	BPW 24		
Remote control Low speed data transmission < 10 MHz, clear package	BPW 34, BPW 46, BPV 10		
IR filter for λ > 900 nm included	BPV 20 F–BPV 23 F, BPW 41 N, S 186 P, BPV 10 F, S 288 P, TFM-Series (with integrated amplifier and demodulator)		
IR filter for λ > 820 nm included	BPV 23 NF, BPW 82, BPW 83		
Fiber optical receiver	frequencies < 20 MHz BPW 88, BPW 24 R		high frequencies BPW 97
Densitometry	BPW 34, BPV 10, BPW 43	BPW 20 R, BPW 21 R	
Quadrant detector		S 239 P	

Phototransistor Circuits

A phototransistor typically is operated in a circuit as shown in figure 32. The resistor R_B can be omitted in most applications. In some phototransistors, the base is not connected. R_B can be used to suppress background radiation by setting a threshold level (see equation 5.1 and 5.2)

$$V_O = V_S – B \times \phi_e \times s(\lambda) \times R_L \qquad (5.1)$$

$$V_O \approx V_S – (B \times \phi_e \times s(\lambda) – 0.6/R_B) \times R_L \qquad (5.2)$$

For the dependence of the rise and fall times on the load resistance and collector-base capacitance refer to chapter ’Properties of Silicon Phototransistors’.

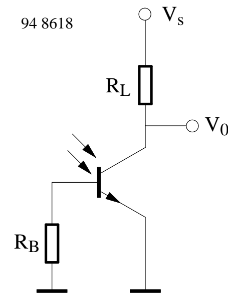

Figure 32. Phototransistor with load resistor and optional base resistor.

Measurement Techniques

Introduction

The characteristics of optoelectronics devices given in the data sheets are verified either by 100% production tests followed by statistic evaluation or by sample tests on typical specimens. These tests can be divided into the following categories:

a) Dark measurements
b) Light measurements
c) Measurements of switching characteristics, cut-off frequency and capacitance
d) Angular distribution measurements
e) Spectral distribution measurements
f) Thermal measurements.

The dark and light measurements are 100% measurements. All other values are typical. The basic circuits used for these measurements are shown in the following sections. The circuits may be modified slightly to cater for special measurement requirements.

Most of the test circuits may be simplified by use of a Source Measure Unit (SMU), which allows either to source voltage and measure current or to source current and measure voltage.

Dark and Light Measurements

Emitter Devices

IR diodes (GaAs)

The forward voltage, V_F, is measured either on a curve tracer or statically using the circuit shown in figure 33. A specified forward current (from a constant current source) is passed through the device and the voltage developed across it is measured on a high-impedance voltmeter.

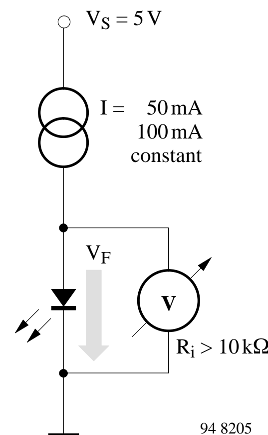

Figure 33.

To measure the reverse voltage, V_R, a 10 µA or 100 µA reverse current from a constant current source is impressed through the diode (figure 34) and the voltage

developed across it is measured on a voltmeter of high input impedance (≥ 10MΩ).

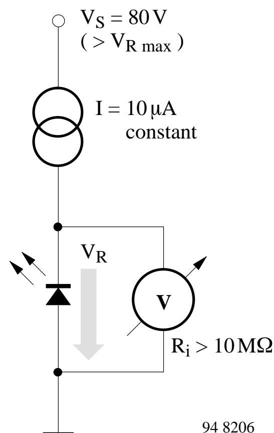

Figure 34.

For most devices, V_R is specified at 10 µA reverse current. In this case either a high impedance voltmeter has to be used, or the current consumption of the DVM has to be calculated and added to the specified current. A second measurement step will then give correct readings.

In the case of GaAs IR diodes, the total radiant output power, Φ_e, is usually measured. This is done with a calibrated large-area photovoltaic cell fitted in a conical reflector with a bore which accepts the test item – see figure 35. An alternative test set uses a silicon photodiode attached to an integrating sphere. A constant dc or pulsating forward current of specified magnitude is passed through the IR diode. The advantage of pulse-current measurements at room temperature (25°C) is that the results can be reproduced exactly. .

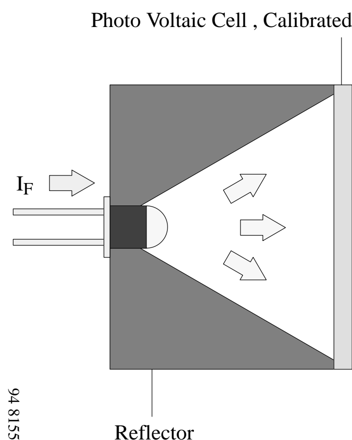

Figure 35.

If, for reasons of measurement economy, only dc measurements (figure 36) are to be made, then the energizing time should be kept short (below 1 s) and of uniform duration, to minimize any fall-off in light output due to internal heating

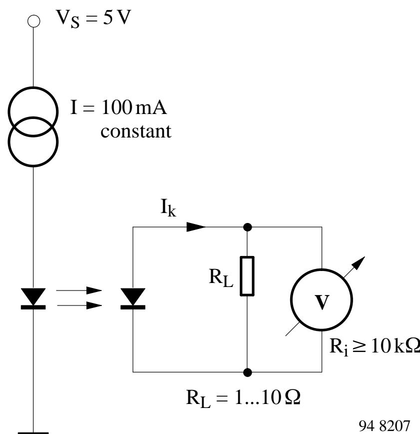

Figure 36.

To ensure that the relationship between irradiance and photocurrent is linear, the photodiode should operate near short-circuit configuration. This can be achieved by using a low resistance load (≤ 10 Ω) of such a value that the voltage dropped across it is very much lower than the open circuit voltage produced under identical illumination conditions ($R_{meas} \ll R_i$).The voltage across the load should be measured with a sensitive DVM.

Knowledge of the radiant intensity, I_e, produced by an IR emitter enables customers to assess the range of IR light barriers. The measurement procedure for this is more or less the same as that used for measuring the radiant power. The only difference is that in this case the photodiode is used without a reflector and is mounted at a specified distance from, and on the optical axis of, the IR diode (figure 37) so that only radiant power of a narrow axial beam is considered. The radiant power within a solid angle of $\Omega = 0.01$ steradian (sr) is measured at a distance of 100 mm. The radiant intensity is then obtained by using this measured value for calculating the radiant intensity for a solid angle of $\Omega = 1$ sr.

Light emitting diodes

For forward and reverse voltage measurements (V_F and V_R respectively) refer to section 'IR diodes (GaAs)'.

The luminous intensity, I_v of a light emitting diode can be calculated by multiplying the radiant intensity, I_e, (figure 37) by the absolute eye sensitivity, $K_m \times V_{(\lambda)}$ (DIN 5031). This assumes, however, that the wavelength of the radiation emitted by the test item is known exactly. In production measurements, a calibrated silicon photovoltaic cell is used in conjunction with a special color filter (e.g., Schott BG 38) which simulates the red-slope of the eye sensitivity curve. BPW20R is used as a photovoltaic cell because the short circuit output current characteristic of this cell is strictly linear even when the

irradiation is very low. This is because the radiant output power of LEDs is low in comparison with that of IR diodes, and the color filter has an attenuating effect causing the cell to produce, at the most, only a few nanoamperes. The cell must operate into an operational amplifier with a high-impedance FET input stage (figure 38). Alternatively a high sensitive electrometer may be used.

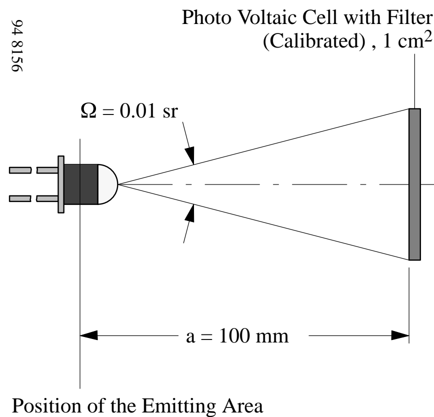

Figure 37.

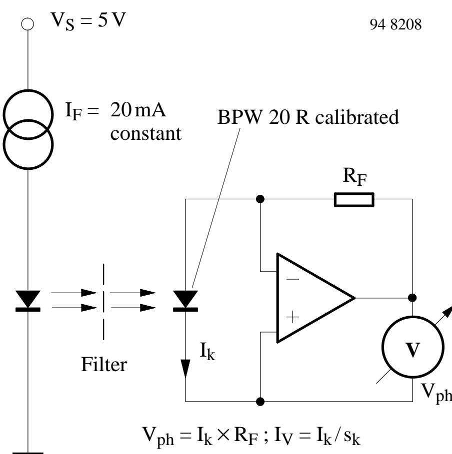

Figure 38.

Detector Devices

Photovoltaic cells, photodiodes

a) Dark measurements

The reverse voltage characteristic, V_R, is measured either on a curve tracer or statically using the circuit shown in figure 39. A high-impedance voltmeter, which draws only an insignificant fraction of the device's reverse current, must be used.

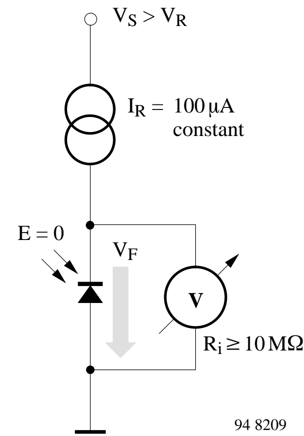

Figure 39.

Dark reverse current measurements, I_{ro}, must be carried out in complete darkness – the reverse currents of silicon photodiodes are of the order of nanoamperes only, and an illumination of a few lux is quite sufficient to falsify the test result. If a highly sensitive DVM is to be used, then a current sampling resistor of such a value that the voltage dropped across it is small in comparison with the supply voltage must be connected in series with the test item (figure 40). Under these conditions, any reverse voltage variations of the test samples can be ignored. Shunt resistance (dark resistance) is determined by applying very slight voltage to the photodiode and then measuring the dark current. In the case of 10 mV or less, forward and reverse polarity will result in similar readings.

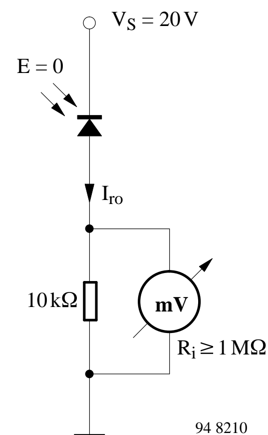

Figure 40.

b) Light measurements

The same circuit used in the dark measurement can be used to carry out light reverse current, I_{ra}, measurements on photodiodes. The only difference is that the diode is now irradiated and a current sampling resistor of lower value must be used (figure 41), because of the higher currents involved.

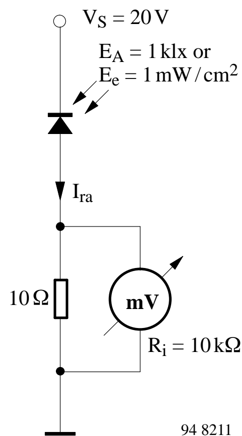

Figure 41.

The open circuit voltage, V_o, and short circuit current, I_k, of photovoltaic cells and photodiodes are measured by means of the test circuit shown in figure 42. The value of the load resistor used for the I_k measurement should be chosen so that the voltage dropped across it is low in comparison with the open circuit voltage produced under conditions of identical irradiation.

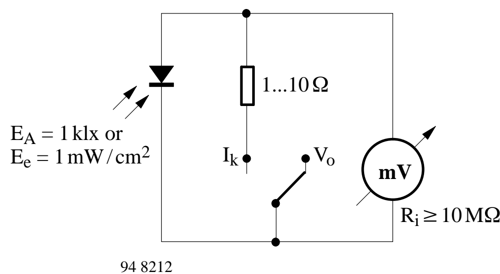

Figure 42.

The light source used for light measurements is a calibrated incandescent tungsten lamp with no filters. The filament current is adjusted for a color temperature of 2856 K (standard illuminant A to DIN 5033 sheet 7), and the specified illumination, E_v, (usually 100 or 1000 lux) is produced by adjusting the distance, a, between the lamp and the detector on an optical bench. E_v can be measured on a V(λ)-corrected luxmeter, or, if the luminous intensity, I_v, of the lamp is known, E_v can be calculated using the formula: $E_v = I_v/a^2$.

It should be noted that this inverse square law is only strictly accurate for point light sources, that is for sources where the dimensions of the source (the filament) are small (≤ 10%) in comparison with the distance between source and detector.

Since lux is a measure for visible light only, near infrared radiation (800 to 1100 nanometers) where silicon detectors have their peak sensitivity, is not taken into account. Unfortunately, near infrared emission of filament lamps of various construction varies widely. As a result, light current measurements carried out with different lamps (but the same lux and color temperature calibration) may result in readings that differ up to 20%.

The simplest way to overcome this problem is to calibrate (measure the light current) some items of a photodetector type with a standard lamp (OSRAM WI 41 / G) and then use these devices for adjustment of the lamp used for field measurements.

An IR diode is used as a radiation source (instead of the tungsten incandescent lamp), to measure detector devices being used mainly in IR transmission systems together with IR emitters (e.g., IR remote control, IR headphone). Operation is possible both with dc or pulsed current.

The adjustment of irradiance, E_e, is similar to the above mentioned adjustment of illuminance, E_v. To achieve a high stability similar to the filament lamps, consideration should be given to the following two points:

- The IR emitter should be connected to a good heat sink to provide sufficient temperature stability.
- dc or pulse-current levels as well as pulse duration have great influence on the self-heating of IR diodes and should be chosen carefully.
- The radiant intensity, I_e, of the device is permanently controlled by a calibrated detector.

Phototransistors, photodarlington transistors

The collector emitter voltage, V_{CEO}, is measured either on a transistor curve tracer or statically using the circuit shown in figure 43. Normal bench illumination does not change the measured result.

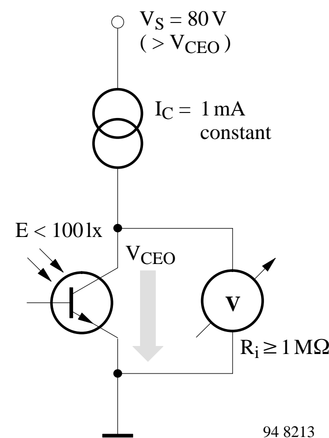

Figure 43.

In contrast, however, the collector dark current, I_{CEO} or I_{co}, must be measured in complete darkness (figure 44). Even ordinary daylight illumination of the wire fed-through glass seals would falsify the measurement result.

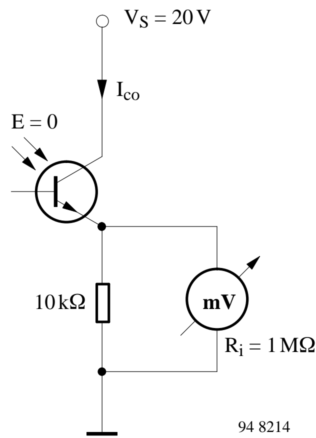

Figure 44.

The same circuit is used for collector light current, I_{ca}, measurements (figure 45), the device being positioned so that its optical axis points towards an incandescent tungsten lamp with no filters, producing a standard-A illuminance of 100 or 1000 lx with a color temperature of T_f = 2856 K. Alternatively an IR irradiance by a GaAs diode is used (refer to the photovoltaic cells and photodiodes section). Note that a lower value sampling resistor is used, in keeping with the higher current involved.

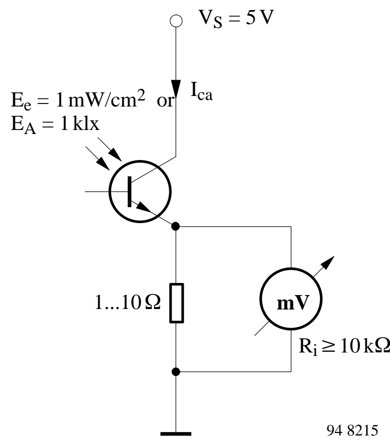

Figure 45.

To measure the collector emitter saturation voltage, V_{CEsat}, the device is illuminated and a constant collector current passed through it. The magnitude of this current is adjusted so that it is less than the minimum light current, $I_{ca\ min}$, for the same illuminance (figure 46). The saturation voltage of the phototransistor or Darlington stage (approximately 100 mV or 600 mV, respectively) is then measured on a high impedance voltmeter.

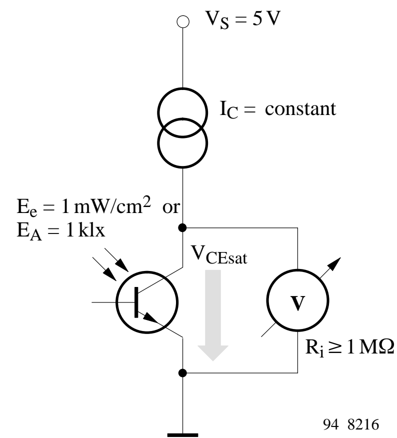

Figure 46.

Switching Characteristics

Definition

Each electronic device generates a certain delay between input and output signals as well as a certain amount of amplitude distortion. A simplified circuit (figure 47) shows how the input and output signals of optoelectronic devices can be displayed on a dual-trace oscilloscope.

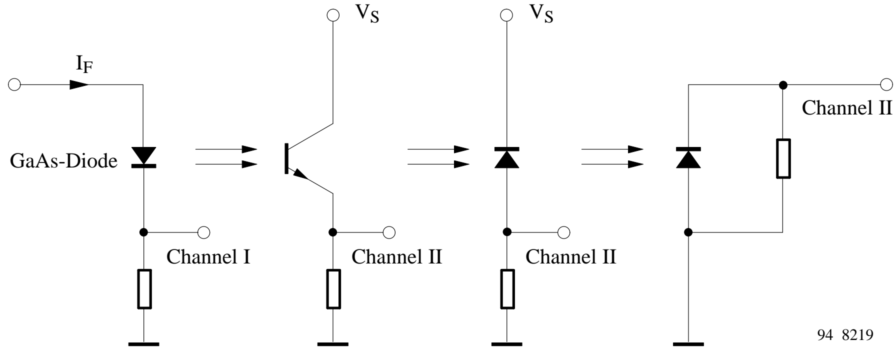

Figure 47.

The switching characteristics can be determined by comparing the timing of the output current waveform with that of the input current waveform (figure 48).

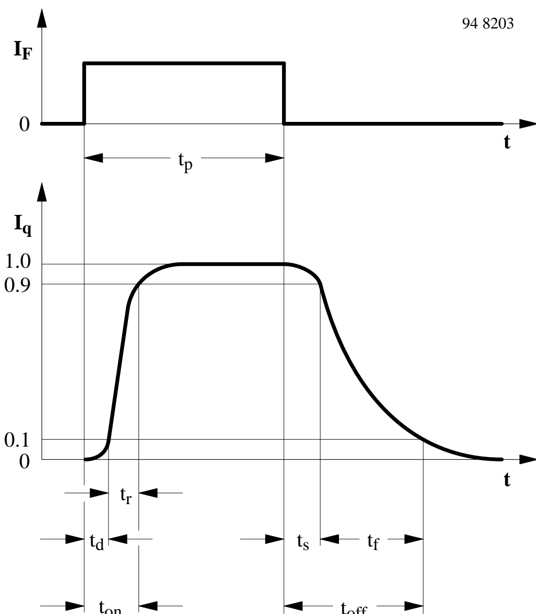

Figure 48.

These time parameters also include the delay that exists in a luminescence diode between the forward current (I_F) and the radiant power (Φ_e).

Notes Concerning the Test Set-up

The circuits used for testing light emitting, light sensitive and optically coupled isolator devices are basically the same (figure 47), the only difference being the way in which the test item is connected in the circuit.

It is assumed that the rise and fall times associated with the signal source (pulse generator) and the dual trace oscilloscope are insignificant, and that the switching characteristics of any light sensitive device used in the set-up are considerably shorter than those of the test item. The switching characteristics of light and IR emitters, for example ($t_r \approx$ 10 to 1000 ns) are measured with the aid of a pin photodiode as a detector ($t_r \approx 1$ ns).
Photo- and darlington transistors and photo- and solar cells ($t_r \approx$ 0.5 to 50 µs) are, as a rule, measured by use of fast IR diodes ($t_r < 30$ ns) as emitters.

GaAsP red light-emitting diodes are used as light sources only for devices which cannot be measured with IR diodes because of their spectral sensitivity (e.g. BPW21R). This is because these diodes emit only 1/10 of the radiant power of IR diodes and consequently generate only very low signal levels.

Switching Characteristic Improvements on Phototransistors and Darlington Phototransistors

As in any ordinary transistor, switching times are reduced if the drive signal level, and hence the collector current, is increased. Another time reduction (especially in fall time t_f) can be achieved by use of a suitable base resistor, assuming there is an external base connection, although this can only be done at the expense of sensitivity.

Component Construction

Infrared components are available in plastic or metal packages.
Plastic devices, where the chip is mounted and bonded on a lead frame are lower in cost and have enhanced output power or sensitivity.
Devices in hermetically sealed packages have better performance in optical and mechanical tolerances and an extended operating temperature range.

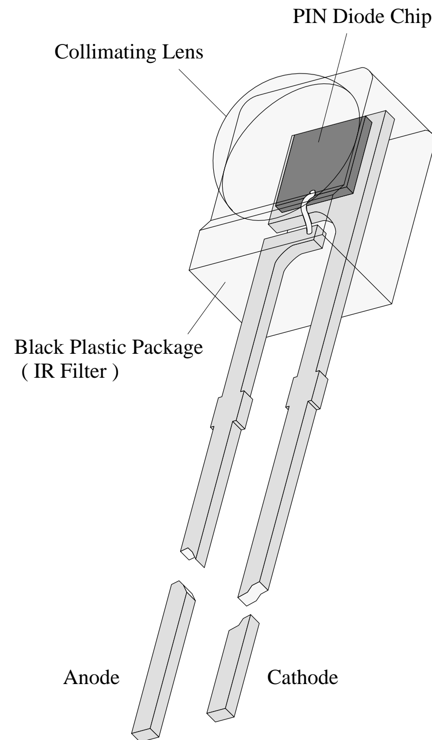

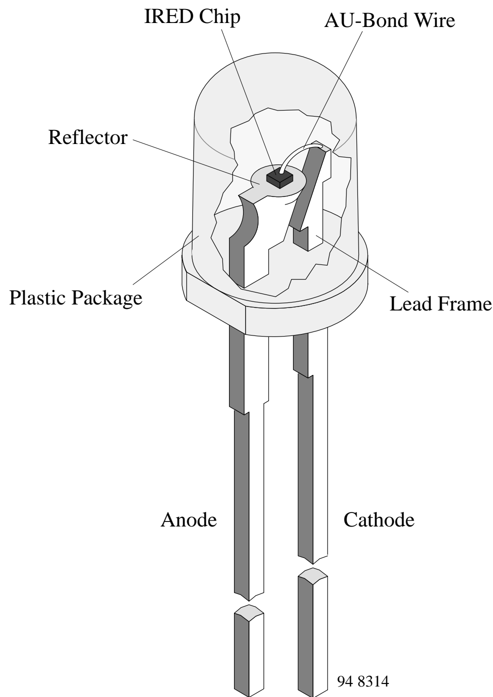

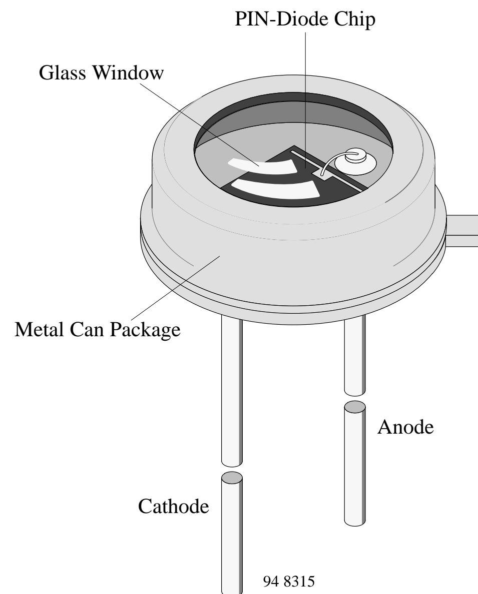

Tape and Reel Standards

TEMIC offers T-1 (3 mm) and T-1$^{3}/_{4}$ (5 mm) IR emitters and detectors packaged on tape. The following specification is based on IEC publication 286, taking into account the industrial requirements for automatic insertion.

Absolute maximum ratings, mechanical dimensions, optical and electrical characteristics for taped devices are identical to the basic catalog types and can be found in the specifications for untaped devices.

Note that the lead wires of taped components may be shorted or bent in accordance with the IEC standard.

Packing

The tapes of components are available on reels or in fan-fold boxes. Each reel and each box is marked with labels which contain the following information:

– Tfk
– Type
– Group
– Tape code (see figure 49)
– Production code
– Quantity

Code for taped IREDs

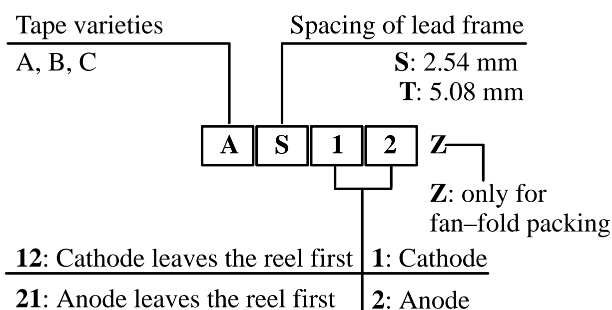

Figure 49. Taping code

Number of Components

Quantity per reel: 3 mm IRED: 2000 pcs
5 mm IRED: 1000 pcs

Quantity per fan-fold box: 3 mm IRED: 2000 pcs
5 mm IRED: 1000 pcs

This results in the increments for the ordering quantities:

3 mm: Increments of 2000 pcs
5 mm: Increments of 1000 pcs

Missing Components

Up to 3 consecutive components may be missing if the gap is followed by at least 6 components. A maximum of 0.5% of the components per reel quantity may be missing. At least 5 empty positions are present at the start and the end of the tape to enable tape insertion.

Tensile strength of the tape: $\geqq$ 15 N

Pulling force in the plane of the tape, at right angles to the reel: $\geqq$ 5 N

Note:
Shipment in fan-fold packages are standard for radial taped devices.
Shipments in reel packing are only possible, if the customer guarantees the removal of empty reels.
According to what is stated in a German packaging decree (Verpackungsverordnung) we are not able to accept the return of reels.

Order Designation

The type designation of the device is extended by the code shown above.

Example: TSIP 5200 AS12 (reel packing) or
TSIP 5200 AS12Z (fan-fold packing)
BPW 85 AS12 (reel packing)

Tape Dimensions for ∅ 3 mm Standard Packages

available package variations: 1 2, 1 2Z, 2 1

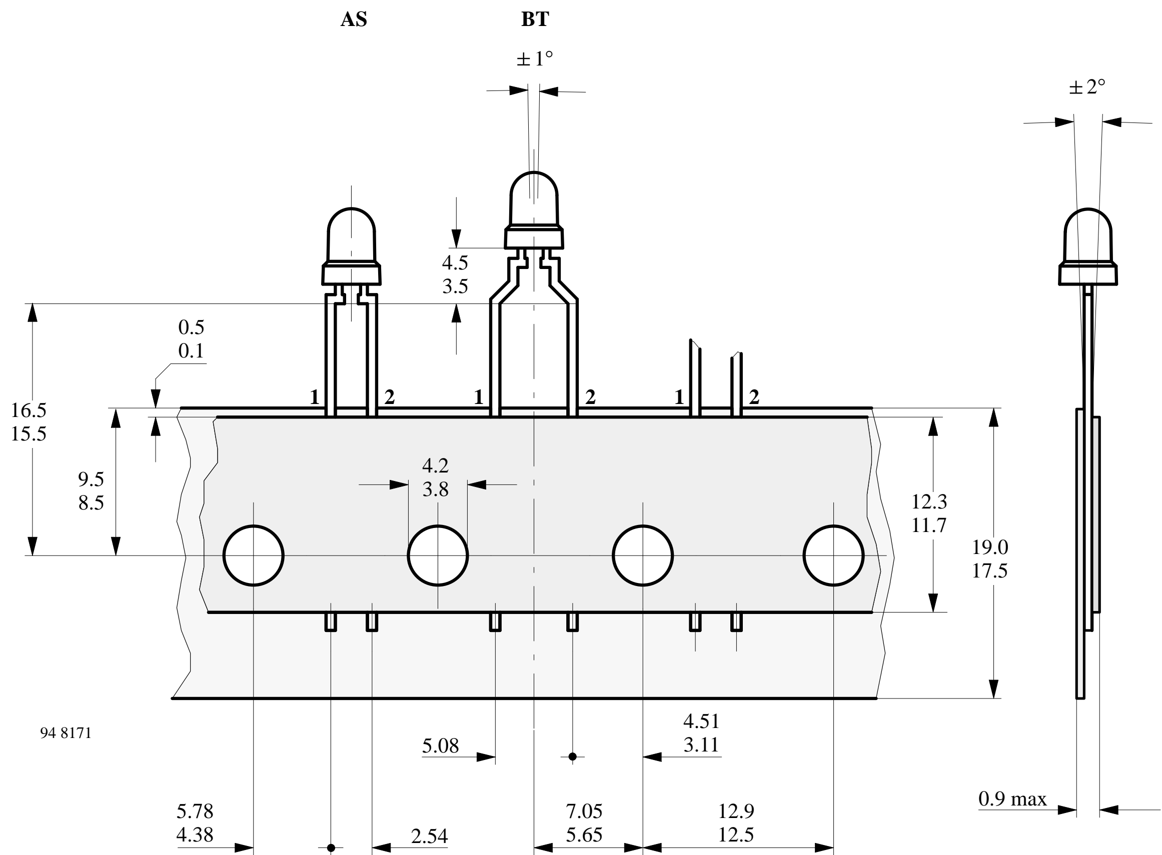

Figure 50. Tape dimensions ∅ 3mm devices

Tape Dimensions for ∅ 5 mm Standard Packages

available package variations: 1 2, 1 2Z, 2 1

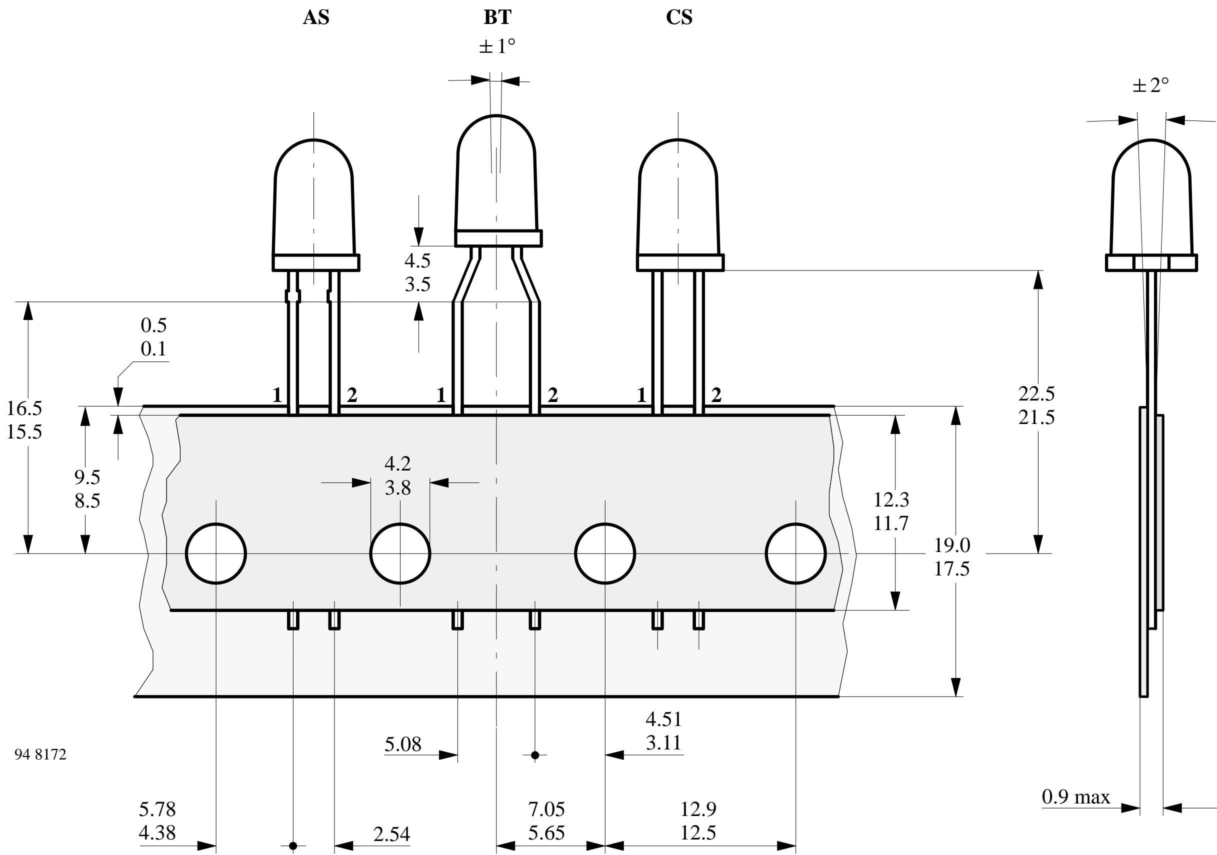

Figure 51. Tape dimensions ∅ 5 mm devices

Reel Package, Dimensions in mm

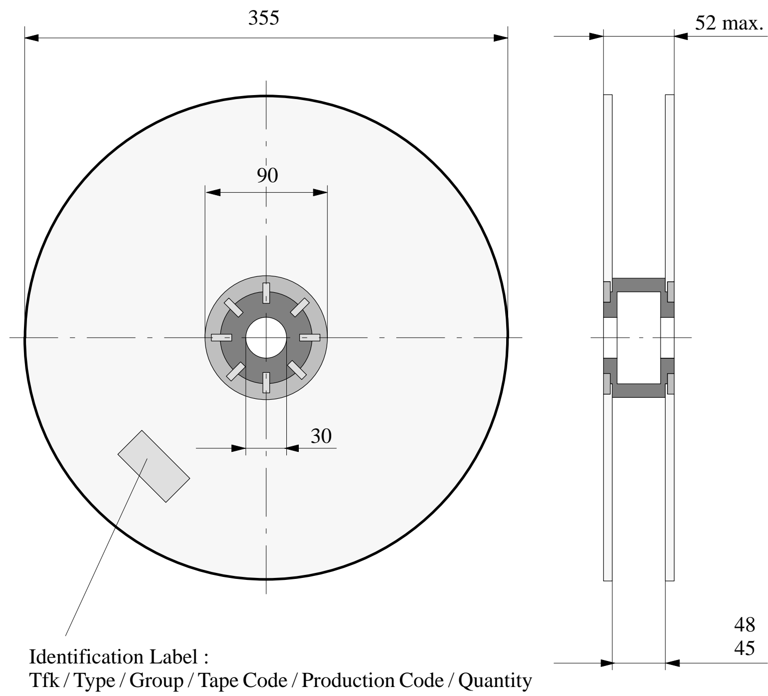

Figure 52. Dimensions of the reel

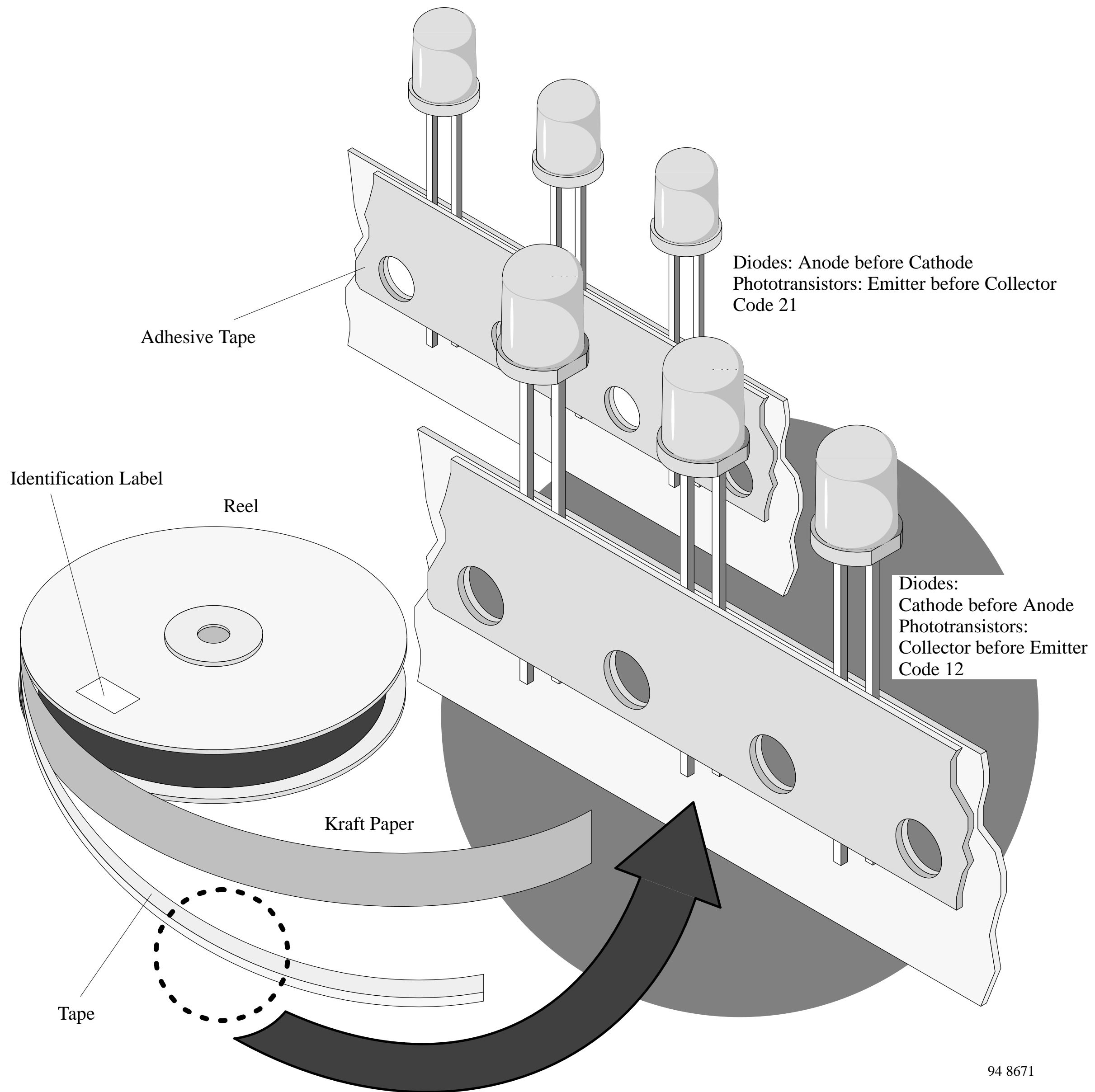

Figure 53. Wound devices

Fan-Fold Packing

The tape is folded in a concertina arrangement and laid in the cardboard box.
If the components are required with the cathode before the anode (figure 54), the start of the tape should be taken from the side of the box marked “–”If the components are required with the anode before cathode, the tape should be taken from the side of the box marked “+”.

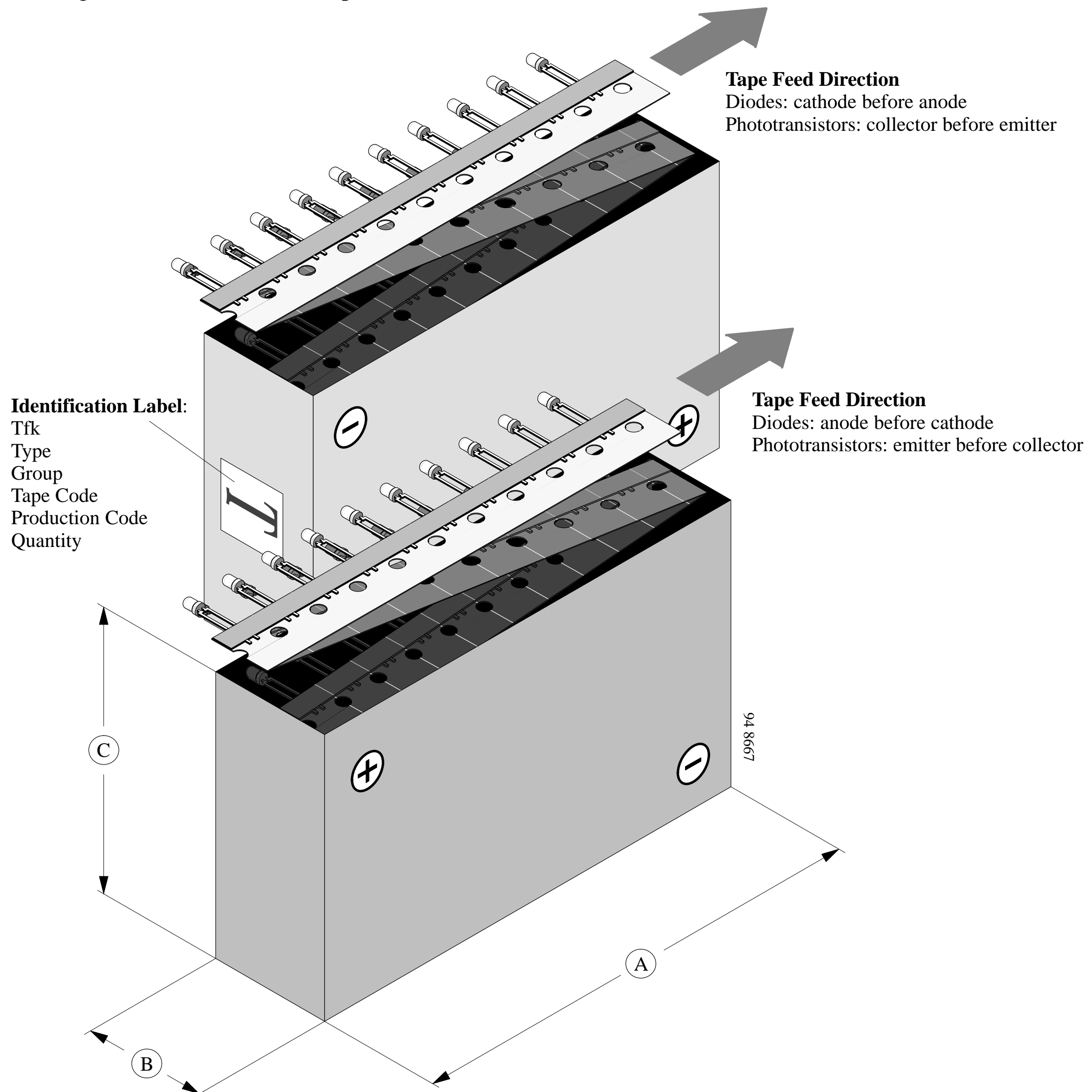

Figure 54. Tape direction

Table 4. Inner dimensions

A	B	C	Packages
340	46	125	∅5 mm
340	34	140	∅3 mm AS-Taping
340	41	140	∅3 mm other than AS-Taping

Taping of SMT-Devices

TEMICs IREDs and detectors in SMD packages are available in an antistatic 8 mm blister tape (in accordance with DIN IEC 40 (CO) 564) for automatic component insertion. The blister tape is a plastic strip with impressed component cavities, covered by a top tape.

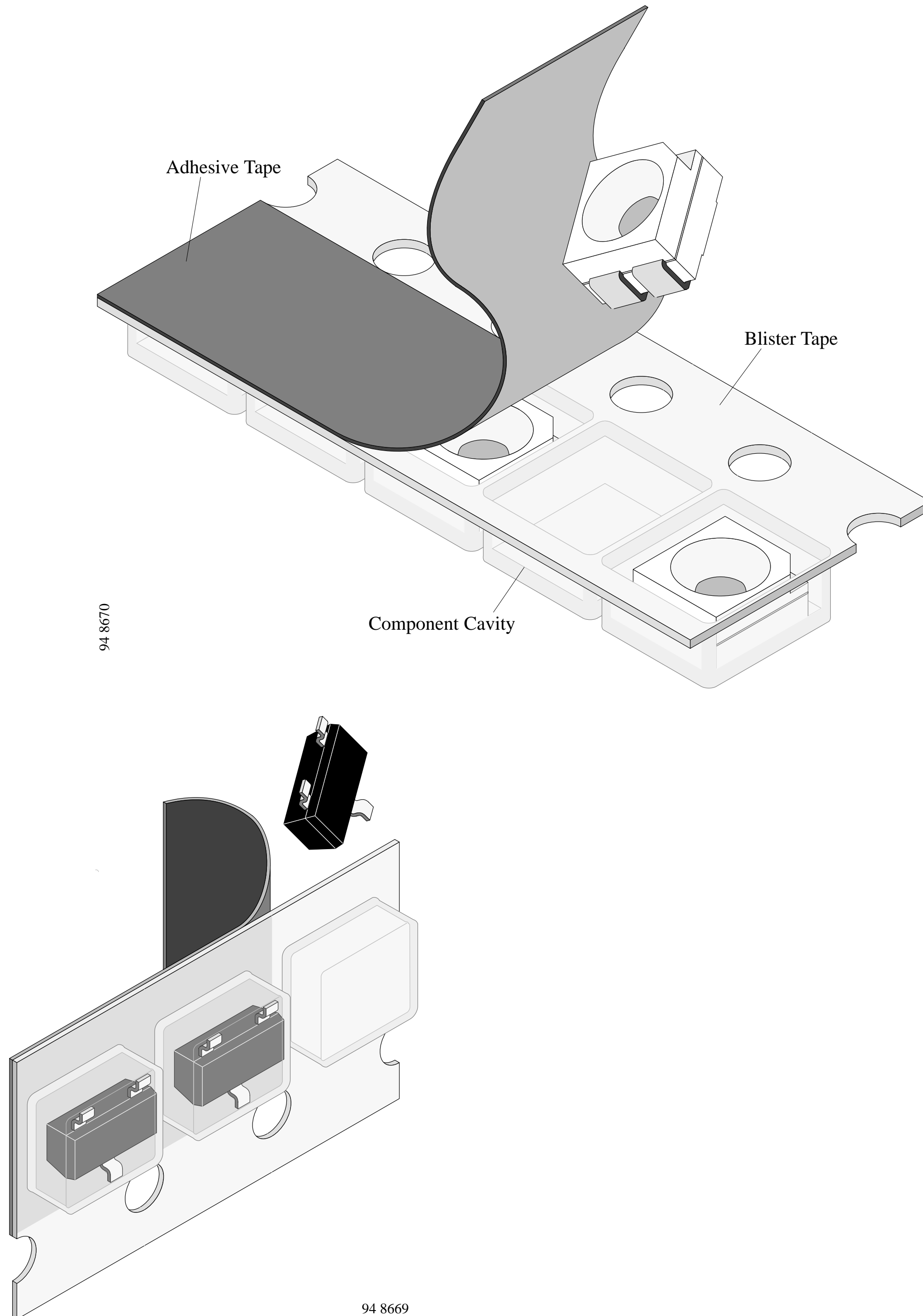

Figure 55. Blister tape

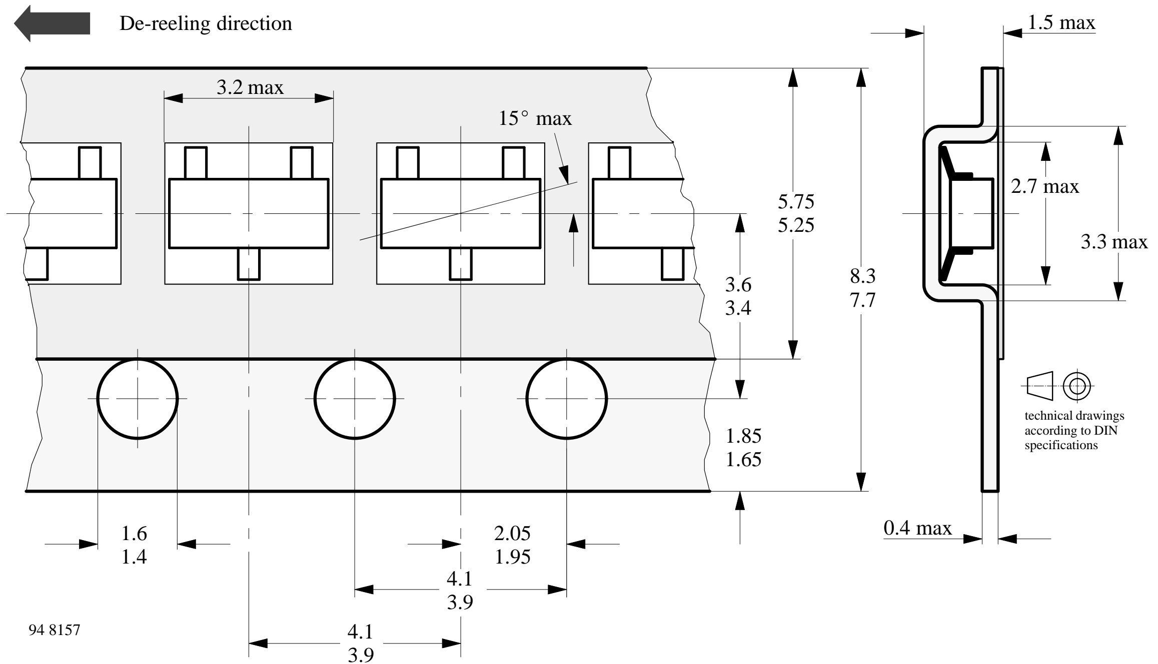

Figure 56. Tape dimensions in mm for SOT 23. The mounting side of the components is oriented to the bottom side in the tape.

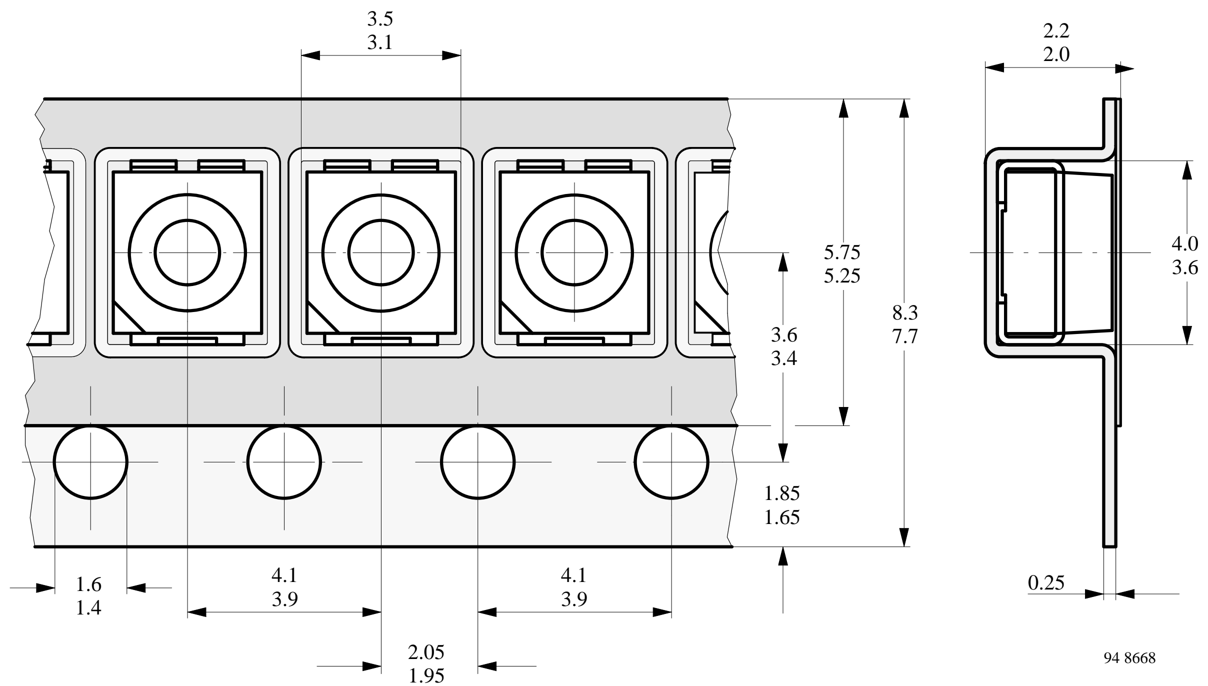

Figure 57. Tape dimensions in mm for PLCC2

Number of Components

Quantity per reel in

SOT 23 package:	3000 pcs
PLCC2 (Tantal B) package:	1500 pcs (minimum quantities for order)

Missing Devices

A maximum of 0.5% of the total number of components per reel may be missing, exclusively missing components at the beginning and at the end of the reel. A maximum of three consecutive components may be missing, provided this gap is followed by six consecutive components.

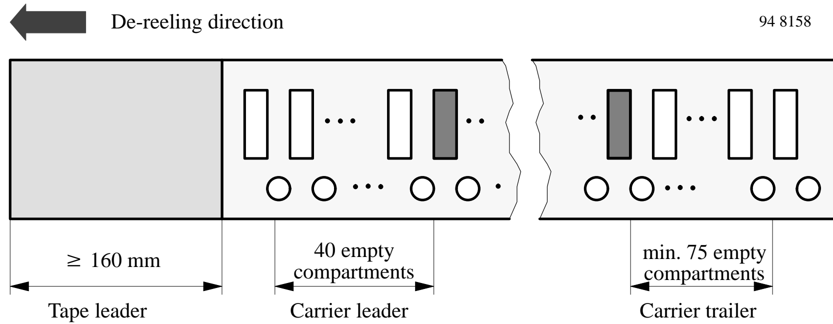

Figure 58. Beginning and end of reel

The tape leader is at least 160 mm and is followed by a carrier tape leader with at least 40 empty compartements. The tape leader may include the carrier tape as long as the cover tape is not connected to the carrier tape.

The last component is followed by a carrier tape trailer with at least 75 empty compartements and sealed with cover tape.

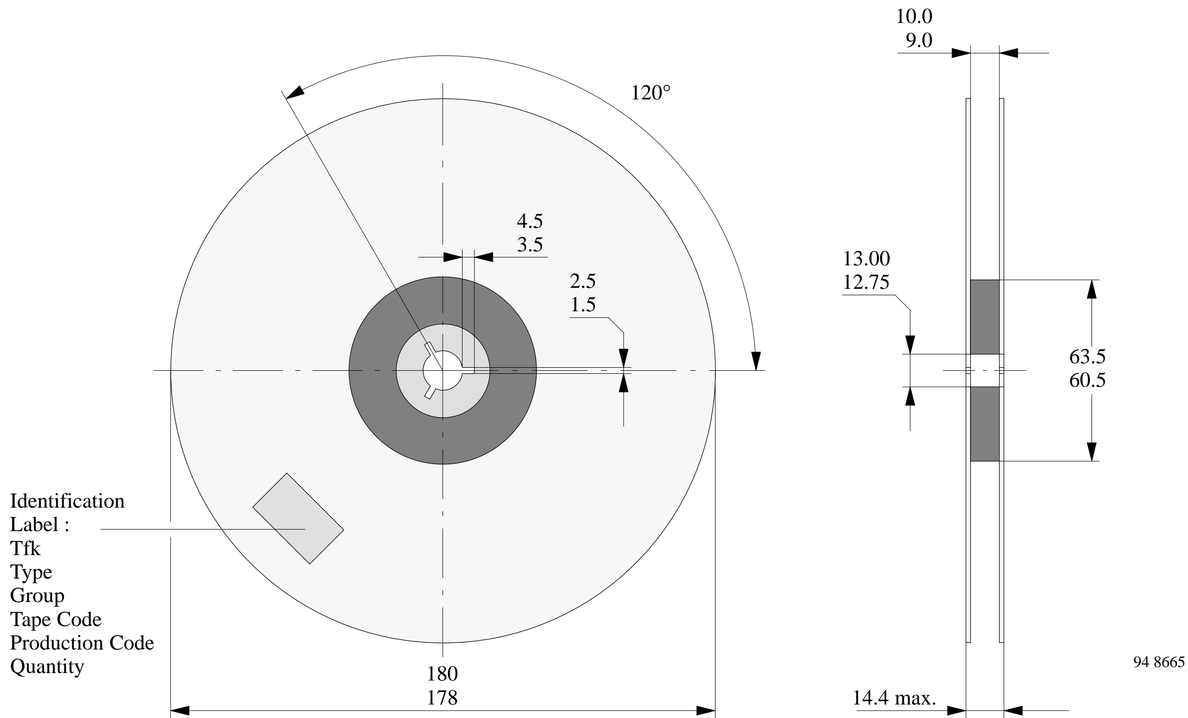

Figure 59. Dimensions of the reel

Cover Tape Removal Force

The removal force lies between 0.1 N and 1.0 N at a removal speed of 5 mm/s.
In order to prevent components from popping out of the blisters, the cover tape must be pulled off at an angle of 180° with regard to the feed direction.

Ordering Designation

The type designation of the device in SOT 23 package is extended by the code GS08.

Example: TEMD 2100 GS08

Assembly instructions

General

Optoelectronic semiconductor devices can be mounted in any position. Connection wires may be bent provided the bend is not less than 1.5 mm from the bottom of the case. During bending, no forces must be transmitted from the pins to the case (e.g., by spreading the pins).

If the device is to be mounted near heat generating components, the resultant increase in ambient temperature should be taken into account.

Soldering instructions

Protection against overheating is essential when a device is being soldered. It is recommended, therefore, that the connection wires are left as long as possible. The time during which the specified maximum permissible device junction temperature is exceeded at the soldering process should be as short as possible (one minute maximum). In the case of plastic encapsulated devices, the maximum permissible soldering temperature is governed by the maximum permissible heat that may be applied to the encapsulant rather than by the maximum permissible junction temperature.

The maximum soldering iron (or solder bath) temperatures are given in Tab. 5. During soldering, no forces must be transmitted from the pins to the case (e.g., by spreading the pins).

Table 5. Maximum Soldering Temperatures

	Iron soldering			Wave soldering		
	Iron temperature	Distance of the soldering position from the lower edge of the case	Maximum allowable soldering time	Soldering temperature see temperature-time profiles	Distance of the soldering position from the lower edge of the case	Maximum allowable soldering time
Devices in metal case	≦245°C ≦245°C ≦350°C	≧1.5 mm ≧5.0 mm ≧5.0 mm	5 s 10 s 5 s	245°C 300°C	≧1.5 mm ≧5.0 mm	5 s 3 s
Devices in plastic case ≥3 mm	≦260°C ≦300°C	≧2.0 mm ≧5.0 mm	5 s 3 s	235°C 260°C	≧2.0 mm ≧2.0 mm	8 s 5 s
Devices in plastic case <3 mm	≦300°C	≧5.0 mm	3 s	260°C	≧2.0 mm	3 s

Soldering Methods

There are several methods in use to solder devices on to the substrate. Some of them are listed in the following:

(a) Soldering in the vapor phase

Soldering in saturated vapor is also known as condensation soldering. This soldering process is used as a batch system (dual vapor system) or as a continuous single vapor system. Both systems may also include preheating of the assemblies to prevent high temperature shock and other undesired effects.

(b) Infrared soldering

With infrared (IR) reflow soldering the heating is contact-free and the energy for heating the assembly is derived from direct infrared radiation and from convection.

The heating rate in an IR furnace depends on the absorption coefficients of the material surfaces and on the ratio of the component's mass to its irradiated surface.

The temperature of parts in an IR furnace, with a mixture of radiation and convection, cannot be determined in advance. Temperature measurement may be performed by measuring the temperature of a certain component while it is beeing transported through the furnace.

The temperatures of small components, soldered together with larger ones, may rise up to 280°C.

Influencing parameters on the internal temperature of the component are as follows:

– Time and power
– Mass of the component
– Size of the component
– Size of the printed circuit board
– Absorption coefficient of the surfaces
– Packing density
– Wavelength spectrum of the radiation source
– Ratio of radiated and convected energy

Temperature-time profiles of the entire process and the influencing parameters are given in figure 60.

(c) Wave soldering

In wave soldering, one or more continuously replenished waves of molten solder are generated, while the substrates to be soldered are moved in one direction across the wave's crest.

Temperature-time profiles of the entire process are given in figure 61.

(d) Iron soldering

This process cannot be carried out in a controlled way. It should not be considered for use in applications where reliability is important. There is no SMD classification for this process.

(e) Laser soldering

This is an excess heating soldering method. The energy absorbed may heat the device to a much higher temperature than desired. There is no SMD classification for this process at the moment.

(f) Resistance soldering

This is a soldering method which uses temperature controlled tools (thermodes) for making solder joints. There is no SMD classification for this process at the moment.

Warning

Devices in PLCC-packages are sensitive to moisture release if they are subjected to infrared reflow or a similar solder process (e.g. wave soldering). After opening the bag, they must be:

1. stored at ambient of <20% relative humidity (RH)
2. used within 2 weeks at factory conditions (<30°C/60% RH)

In case of moisture absorption, the devices will recover to former condition by drying under recommended condition: 60°C / 96 h.

Temperature-Time Profiles

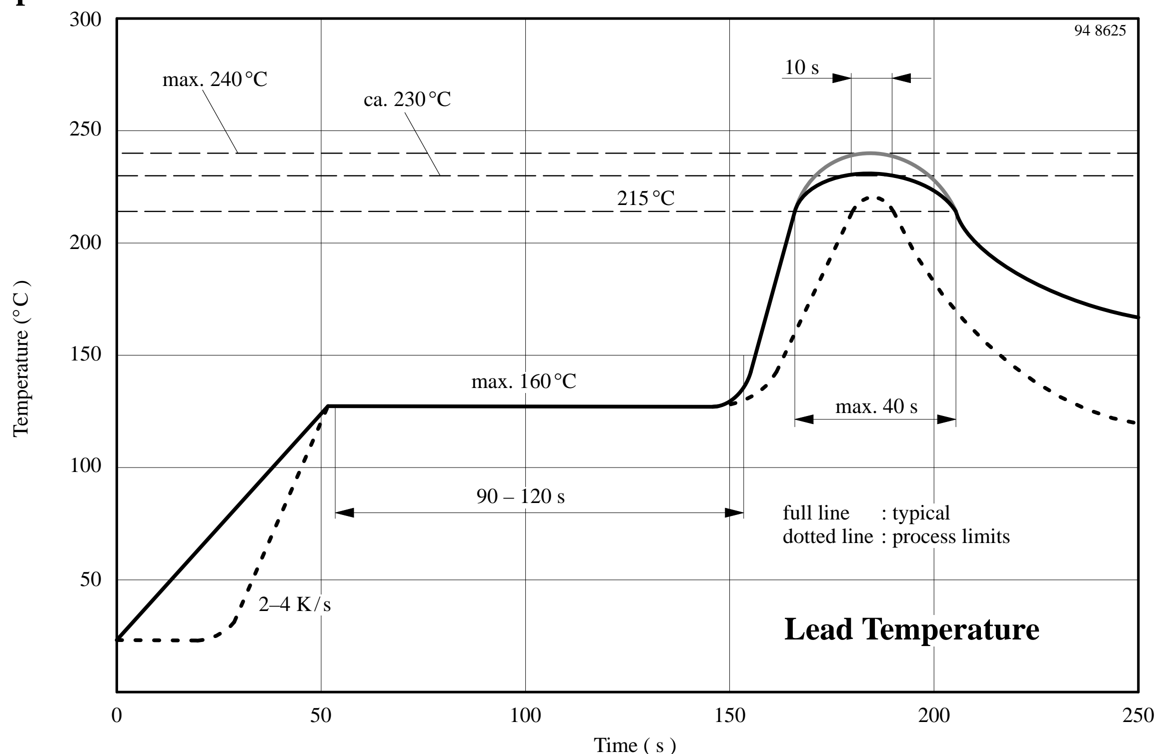

Figure 60. Infrared reflow soldering of opto devices (SMD package)

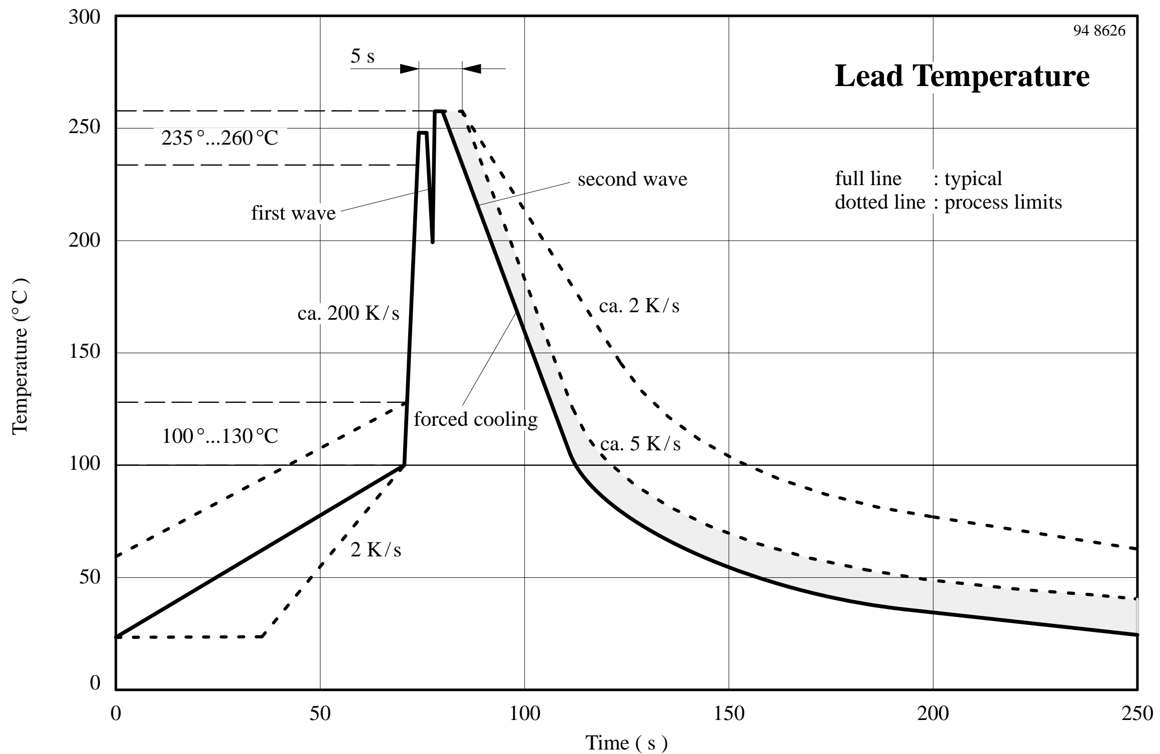

Figure 61. Double wave soldering of opto devices

Heat Removal

To keep the thermal equilibrium, the heat generated in the semiconductor junction(s) must be removed and the junction returned to ambient temperature.

In the case of low power devices, the natural heat conductive path between the case and surrounding air is usually adequate for this purpose. The heat generated in the junction is conveyed to the case or header by conduction rather than convection. A measure of the effectiveness of heat conduction is the inner thermal resistance or thermal resistance junction case, R_{thJC}, the value of which is governed by the construction of the device.

Any heat transfer from the case to the surrounding air involves radiation convection and conduction, the effectiveness of transfer being expressed in terms of an R_{thCA} value, i.e., the external or case ambient thermal resistance. The total thermal resistance, junction ambient is consequently:

$$R_{thJA} = R_{thJC} + R_{thCA}$$

The total maximum power dissipation, $P_{tot\ max}$ of a semiconductor device can be expressed as follows:

$$P_{tot\ max} = \frac{T_{jmax} - T_{amb}}{R_{thJA}} = \frac{T_{jmax} - T_{amb}}{R_{thJC} + R_{thCA}}$$

where:

T_{jmax} the maximum allowable junction temperature

T_{amb} the highest ambient temperature likely to be reached under the most unfavorable conditions

R_{thJC} the thermal resistance, junction case

R_{thJA} the thermal resistance, junction ambient, is specified for the components. The following diagram shows how the different installation conditions effect the thermal resistance

R_{thCA} the thermal resistance, case ambient. R_{thCA} depends on cooling conditions. If a heat dissipator or sink is used, R_{thCA} depends on the thermal contact between case and heat sink, heat propagation conditions in the sink and the rate at which heat is transferred to the surrounding air.

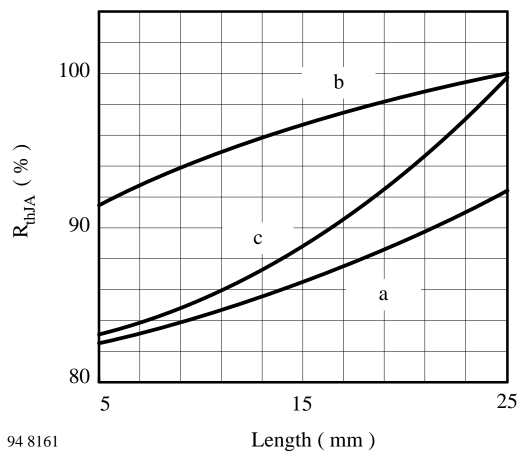

Figure 62. Thermal resistance junction/ambient vs. lead length

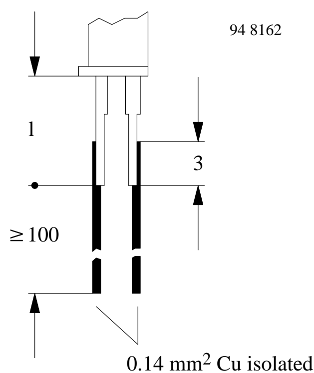

Figure 63. In the case of wire contacts (curve b, figure 62)

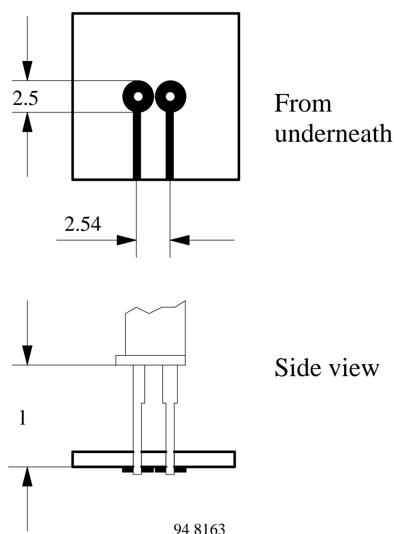

Figure 64. In the case of assembly on PC board, no heatsink (curve c, figure 62)

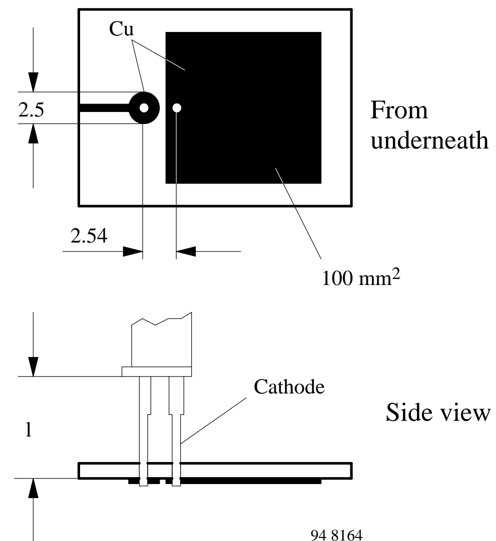

Figure 65. In the case of assembly on PC board with heatsink (curve a, figure 62)

Cleaning

Soldered assemblies are washable with the following solvents:

1) A mixture of 1, 1.2-trichlorotrifluoroethane, 70 ± 5% by weight and 2-propanol (isopropyl alcohol), 30 ± 5% by weight.
   Commercially available grades (industrial use) should be used.

   Warning: The component 1, 1.2-trichlorofluoroethane is hazardous to the environment. Therefore this solvent must not be used where the solvent specified in 2 or 3 is adequate.

2) 2-propanol (isopropyl alcohol).
   Commercially available grades (industrial use) should be used.

3) Demineralized or distilled water having a resistivity of not less than 500 mΩ corresponding to a conductivity of 2 mS/m.

Caution: The use of tetrachlor, acetone, trichloroetylene or similar is **NOT ALLOWED!**

Warning

Exceeding any one of the ratings (soldering, cleaning or short time exceeding the railings) could result in irreversible changes in the ratings.

Quality Information

TEMIC's Continuous Improvement Activities

- Quality training for ALL personnel including production, development, marketing and sales departments
- Zero defect mindset
- Permanent quality improvement process
- Total Quality Management (TQM)
- TEMIC's Quality Policy established by the Management Board
- Quality system certified per ISO 9001 on July 12, 1993 (Commercial Quality System)
- Quality system formerly approved per AQAP-1 (Military Quality System)

TEMIC Tools for Continuous Improvement

- TEMIC qualifies materials, processes and process changes
- TEMIC uses Process FMEA (Failure Mode and Effects Analysis) for all processes. Process and machine capability as well as Gage R&R (Repeatability & Reproducibility) are proven
- TEMIC's internal qualifications correspond to IEC 68–2 and MIL STD 883
- TEMIC periodically requalifies device types (Short Term Monitoring, Long Term Monitoring).
- TEMIC uses SPC for significant production parameters. SPC is performed by trained operators.
- TEMIC's Burn-In of selected device types.
- TEMIC's 100% testing of final products.
- TEMIC's lot release is carried out via sampling. Sampling acceptance criterion is always c = 0.

TEMIC's Quality Policy

Our goal is to achieve total customer satisfaction
through everything we do.
Therefore, the quality of our products and services
is our number one priority.

Quality comes first!

All of us at TEMIC are part of the process of
continuous improvement.

General Quality Flow Chart Diagram

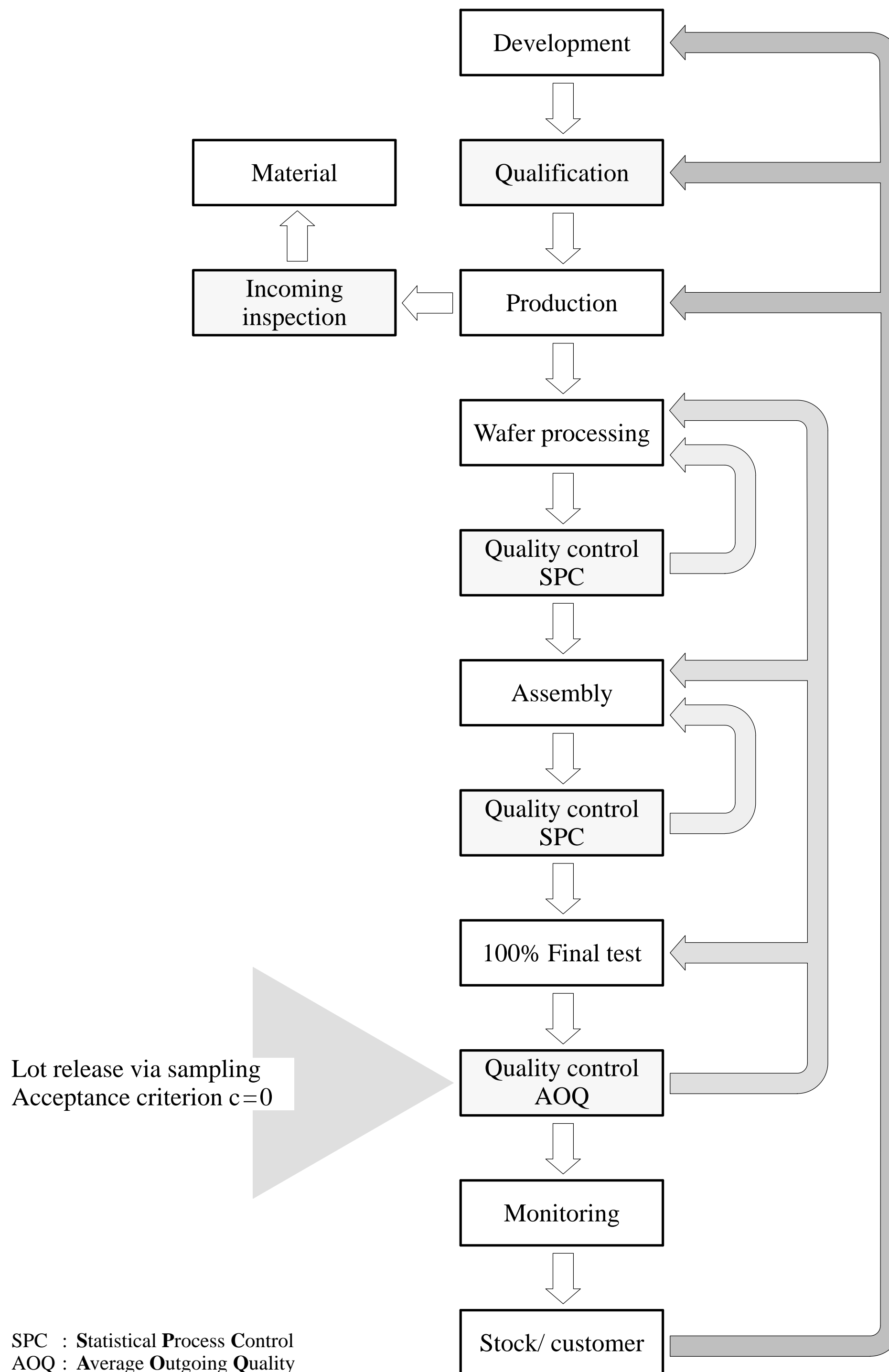

Production Flow Chart Diagram

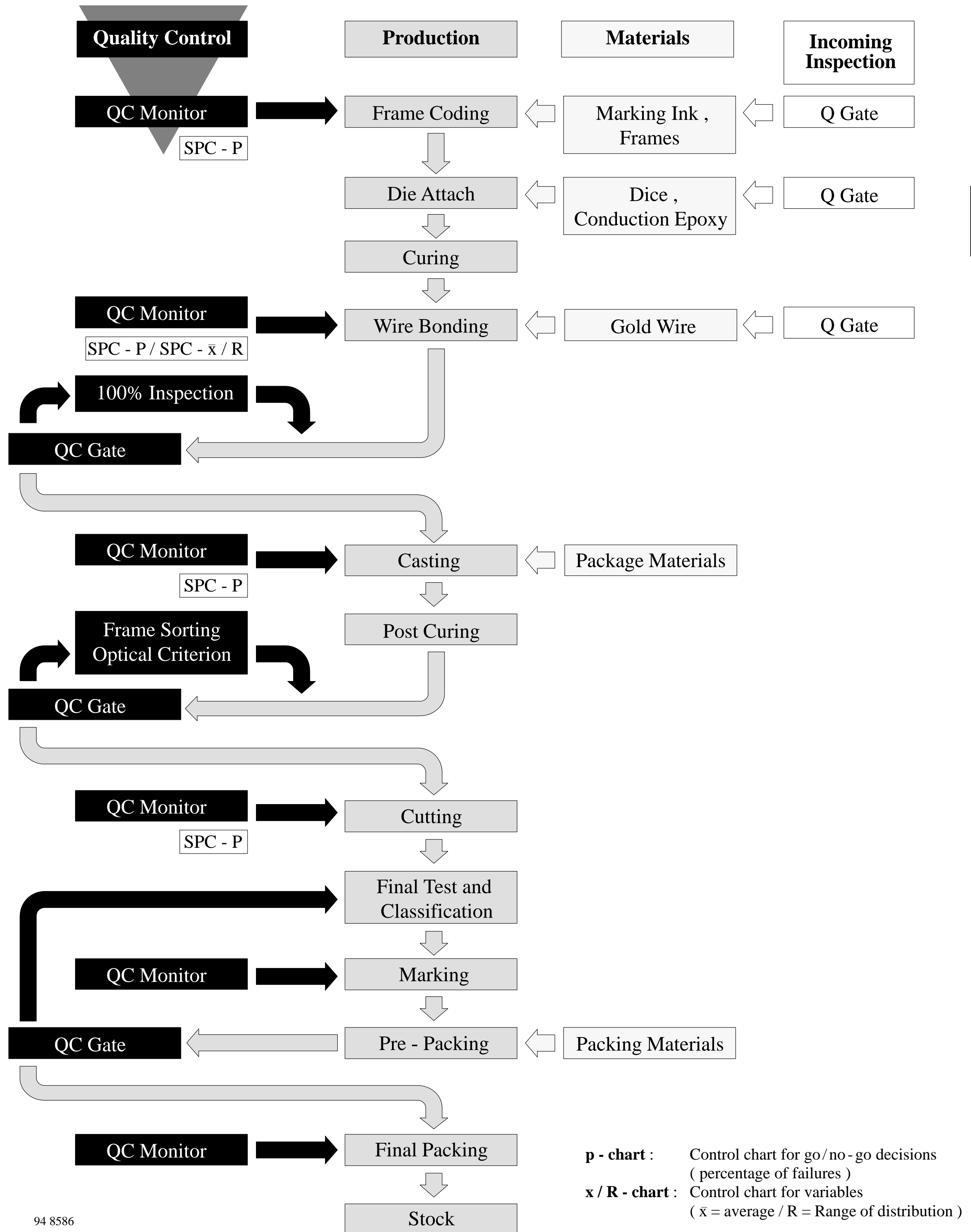

p - chart : Control chart for go / no - go decisions (percentage of failures)

x / R - chart : Control chart for variables (x̄ = average / R = Range of distribution)

Qualification and Release

New wafer processes, packages and device types are qualified according to the internal TEMIC Semiconductors specification QSA 3000.

QSA 3000 consists of five parts (see figure 66).

Wafer process release: The wafer process release is the fundamental release/qualification for the various technologies used by TEMIC Semiconductors. Leading device types are defined fo various technologies. Three wafer lots of these types are subjected to an extensive qualification procedure and are used to represent this technology. A positive result will release the technology.

Package release: The package release is the fundamental release/ qualification for the different packages used. Package groups are defined (see figure 66).

Critical packages are selected: two assembly lots are subjected to the qualification procedure representing that package group. A positive result will release all similar packages.

Device type release: The device type released is the release of individual designs.

Monitoring: Monitoring serves both as the continuous monitoring of the production and as a source of data for calculation of early failures (early failure rate: EFR).

Product or process changes are released via ECN (**E**ngineering **C**hange **N**ote). This includes proving process capability and meeting the quality requirements.

Test procedures utilized are IEC 68–2–... and MIL–STD–883 D respectively.

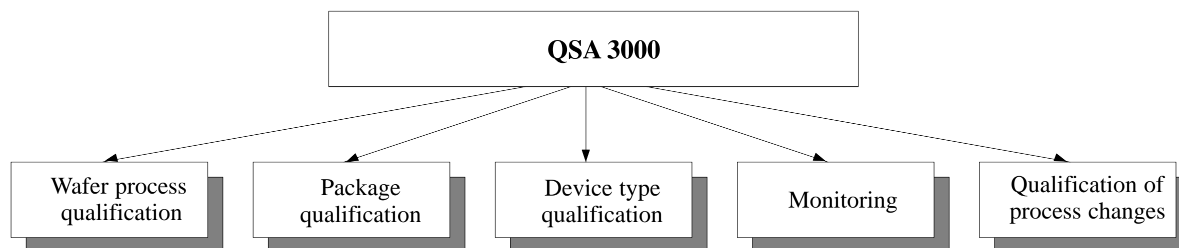

Figure 66. Structure of QSA 3000

Statistical Methods for Prevention

To manufacture high-quality products, it is not sufficient controlling the product at the end of the production process.

Quality has to be ‘designed-in’ during process- and product development. In addition to that, the ‘designing-in’ must also be ensured during production flow. Both will be achieved by means of appropriate measurements and tools.

- Statistical Process Control (SPC)
- R&R– (Repeatability and Reproducibility) tests
- Up– Time Control (UTC)
- Failure Mode and Effect Analysis (FMEA)
- Design Of Experiments (DOE)
- Quality Function Deployment (QFD)

TEMIC Semiconductors has been using SPC as a tool in production since 1990/91.

By using SPC, deviations from the process control goals are quickly established. This allows control of the processes before the process parameters run out of specified limits. To assure control of the processes, each process step is observed and supervised by trained personnel. Results are documented.

Process capabilities are measured and expressed by the process capability index (C_{pk}).

Validation of the process capability is required for new processes before they are released for production.

Before using new equipment and new gauges in production, machine capability (C_{mk} = machine capability index) or R&R (Repeatability & Reproducibility) is used to validate the equipment’s fitness for use.

Up–Time is recorded by an Up–Time Control (UTC) system. This data determines the intervals for preventive maintenance, which is the basis for the maintenance plan.

A process–FMEA is performed for all processes (FMEA = Failure Mode and Effect Analysis). In addition, a de-

sign– or product– FMEA is used for critical products or to meet agreed customer requirements.

Design of Experiments (DOE) is a tool for the statistical design of experiments and is used for optimization of processes. Systems (processes, products and procedures) are analyzed and optimized by using designed experiments.

A significant advantage compared to conventional methods is the efficient perfomance of experiments with minimum effort by determining the most important inputs for optimizing the system.

As a part of the continuous improvement process, all TEMIC Semiconductors' employees are trained in using new statistical methods and procedures.

Reliability

The requirements concerning quality and reliability of products are always increasing. It is not sufficient to only deliver fault–free parts. In addition, it must be ensured that the delivered goods serve their purpose safely and failure free, i.e., reliably. From the delivery of the device and up to its use in a final product, there are some occasions where the device or the final product may fail despite testing and outgoing inspection.

In principle, this sequence is valid for all components of a product.

For these reasons, the negative consequences of a failure, which become more serious and expensive the later they occur, are obvious. The manufacturer is therefore interested in supplying products with the lowest possible

- AOQ (Average Outgoing Quality) value
- EFR (Early Failure Rate) value
- LFR (Long-term Failure Rate) value

Average Outgoing Quality (AOQ)

All outgoing products are sampled after 100% testing. This is known as "Average Outgoing Quality" (AOQ). The results of this inspection are recorded in ppm (parts per million) using the method defined in JEDEC 16.

Early Failure Rate (EFR)

EFR is an estimate (in ppm) of the number of early failures related to the number of devices used. Early failures are normally those which occur within the first 300 to 1000 hours. Essentially, this period of time covers the guarantee period of the finished unit. Low EFR values are therefore very important to the device user. The early life failure rate is heavily influenced by complexity. Consequently, 'designing-in' of better quality during the development and design phase, as well as optimized process control during manufacturing, significantly reduces the EFR value. Normally, the early failure rate should not be significantly higher than the random failure rate. EFR is given in ppm (parts per million).

Long-Term Failure Rate (LFR)

LFR shows the failure rate during the operational period of the devices. This period is of particular interest to the manufacturer of the final product. Based on the LFR value, estimations concerning long-term failure rate, reliability and a device's or module's usage life may be derived. The usage life time is normally the period of constant failure rate. All failures occuring during this period are random.

Within this period the failure rate is:

$$\lambda = \frac{\text{Sum of failures}}{\sum (\text{Quantity} \times \text{Time to failure})} \quad \frac{1}{\text{hours}}$$

The measure of λ is FIT (Failures In Time = number of failures in 10^9 device hours).

Example

A sample of 500 semiconductor devices is tested in a operating life test (dynamic electric operation). The devices operate for a period of 10,000 hours.

Failures: 1 failure after 1000 h
1 failure after 2000 h

The failure rate may be calculated from this sample by

$$\lambda = \frac{2}{1 \times 1000 + 1 \times 2000 + 498 \times 10000} \quad \frac{1}{h}$$

$$\lambda = \frac{2}{4983000} \quad \frac{1}{h} = 4.01 \times 10^{-7} \frac{1}{h}$$

This is a λ-value of 400 FIT, or this sample has a failure rate of 0.04% / 1000 h on average.

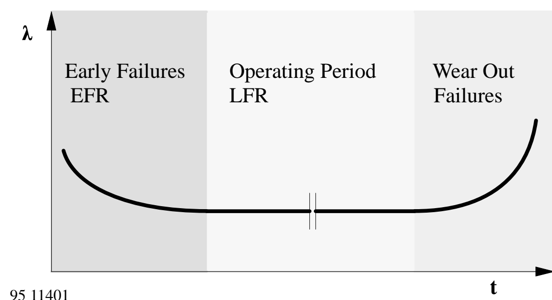

Figure 67. Bath tub curve

Confidence Level

The failure rate λ calculated from the sample is an estimate of the unknown failure rate of the lot.

The interval of the failure rate (confidence interval) may be calculated, depending on the confidence level and sample size.

The following is valid:

- The larger the sample size, the narrower the confidence interval.
- The lower the confidence level of the statement, the narrower the confidence interval.

The confidence level applicable to the failure rate of the whole lot when using the estimated value of λ is derived from the $\varkappa^2$-distribution. In practice, only the upper limit of the confidence interval (the maximum average failure rate) is used.

Therefore:

$$\lambda_{max} = \frac{\varkappa^2/2\ (r; P_A)}{n \times t} \text{ in } \frac{1}{h}$$

$$LFR = \frac{\varkappa^2/2\ (r; P_A)}{n \times t} \times 1 \times 10^9 \text{ in [FIT]}$$

r: Number of failures

P_A: Confidence level

n: Sample size

t: Time in hours

$n \times t$: Device hours

The $\varkappa^2/2$ for λ are taken from table 6.

For the above example from table 6:
$\varkappa^2/2$ (r=2; P_A=60%) = 3.08
$n \times t$ = 4983000 h

$$\lambda_{max} = \frac{3.08}{4983000} = 6.18 \times 10^{-7} \frac{1}{h}$$

This means that the failure rate of the lot does not exceed 0.0618% / 1000 h (618 FIT) with a probability of 60%.

If a confidence level of 90% is chosen from the table 6:
$\varkappa^2/2$ (r=2; P_A=90%) = 5.3

$$\lambda_{max} = \frac{5.3}{4983000} = 1.06 \times 10^{-6} \frac{1}{h}$$

This means that the failure rate of the lot does not exceed 0.106% / 1000 h (1060 FIT) with a probability of 90%.

Table 6.

Number of Failures	Confidence Level			
	50%	**60%**	**90%**	**95%**
0	0.60	0.93	2.31	2.96
1	1.68	2.00	3.89	4.67
2	2.67	3.08	5.30	6.21
3	3.67	4.17	6.70	7.69
4	4.67	5.24	8.00	9.09
5	5.67	6.25	9.25	10.42
6	6.67	7.27	10.55	11.76
7	7.67	8.33	11.75	13.16
8	8.67	9.35	13.00	14.30
9	9.67	10.42	14.20	15.63
10	10.67	11.42	15.40	16.95

Operating Life Tests

Number of devices tested: n = 50

Number of failures (positive qualification): c = 0

Test time: t = 2000 hours

Confidence level: P_A = 60%

$\varkappa^2/2$ (0; 60%) = 0.93

$$\lambda_{max} = \frac{0.93}{50 \times 2000} = 9.3 \times 10^{-6} \frac{1}{h}$$

This means, that the failure rate of the lot does not exceed 0.93% / 1000 h (9300 FIT) with a probability of 60%.

This example demonstrates that it is only possible to verify LFR values of 9300 FIT with a confidence level of 60% in a normal qualification tests (50 devices, 2000 h).

To obtain LFR values which meet today’s requirements (< 50 FIT), the following conditions have to be fulfilled:

- Very long test periods
- Large quantities of devices
- Accelerated testing (e.g., higher temperature)

Mean Time to Failure (MTTF)

For systems which can not be repaired and whose devices must be changed, e.g., semiconductors, the following is valid:

$$MTTF = \frac{1}{\lambda}$$

MTTF is the average fault-free operating period per a monitored (time) unit.

Accelerating Stress Tests

Innovation cycles in the field of semiconductors are becoming shorter and shorter. This means that products must be brought to the market quicker. At the same time, expectations concerning the quality and reliability of the products have become higher.

Manufacturers of semiconductors must therefore assure long operating periods with high reliability but in a short time. Sample stress testing is the most commonly used way of assuring this.

The rule of Arrhenius describes this temperature-dependent change of the failure rate.

$$\lambda(T_2) = \lambda(T_1) \times e^{\left[\frac{E_A}{k} \times \left(\frac{1}{T_1} - \frac{1}{T_2}\right)\right]}$$

Boltzmann's constant
$k = 8.63 \times 10^{-5}$ eV/K

Activation energy
E_A in eV

Junction temperature real operation
T_1 in Kelvin

Junction temperature stress test
T_2 in Kelvin

Failure rate real operation
$\lambda\ (T_1)$

Failure rate stress test
$\lambda\ (T_2)$

The acceleration factor is described by the exponential function as being:

$$AF = \frac{\lambda(T_2)}{\lambda(T_1)} = e^{\left[\frac{E_A}{k} \times \left(\frac{1}{T_1} - \frac{1}{T_2}\right)\right]}$$

Example

The following conditions apply to an operating life stress test:

Environmental temperature during stress test
$T_A = 70°C$

Power dissipation of the device
$P_V = 100$ mW

Thermal resistance junction/environment
$R_{thJA} = 300$ K/W

The system temperature / junction temperature results from:

$$T_J = T_A + R_{thJA} \times P_V$$

$$T_J = 70°C + 300\ K/W \times 100\ mW$$

$$T_J = 100°C$$

Operation in the field at an ambient temperature of 50°C and at an average power dissipation of 80 mW is utilized. This results in a junction temperature in operation of $T_J = 74°C$. The activation energy used for opto components is $E_A = 0.8$ eV.

The resulting acceleration factor is:

$$AF = \frac{\lambda(373K)}{\lambda(347K)} = e^{\left[\frac{E_A}{k} \times \left(\frac{1}{347K} - \frac{1}{373K}\right)\right]}$$

$$AF \approx 6.5$$

This signifies that, regarding this example, the failure rate is lower by a factor of 6.5 compared to the stress test.

Other accelerating stress tests may be:

- Humidity (except displays type TDS.)
  $T_A = 85°C$
  RH = 85%
- Temperature cycling
  Temperature interval as specified

The tests are carried out according to the requirements of appropriate IEC–standards (see also chapter 'Qualification and Release').

Activation Energy

There are some conditions which need to be fulfilled in order to use Arrhenius' method:

- The validity of Arrhenius' rule has to be verified.
- 'Failure-specific' activation energies must be determined.

These conditions may be verified by a series of tests. Today, this procedure is generally accepted and used as a basis for estimating operating life. The values of activation energies can be determined by experiments for different failure mechanisms.

Values often used for different device groups are:

Opto components	0.8 eV
Bipolar ICs	0.7 eV
MOS ICs	0.6 eV
Transistors	0.7 eV
Diodes	0.7 eV

By using this method, it is possible to provide long–term predictions for the actual operation of semiconductors even with relatively short test periods.

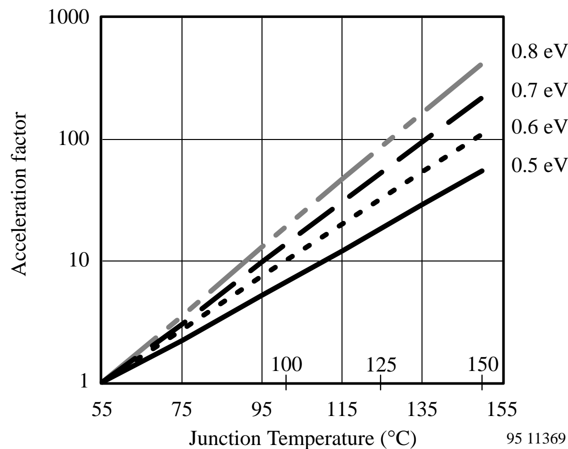

Figure 68. Acceleration factor for different activation energies normalized to $T_j = 55°C$

Degradation of IREDs

The diagrams in figure 69 and figure 70 are based on electrical life tests, calculated with $E_a = 0.8$ eV at $T_j = 25°C$.

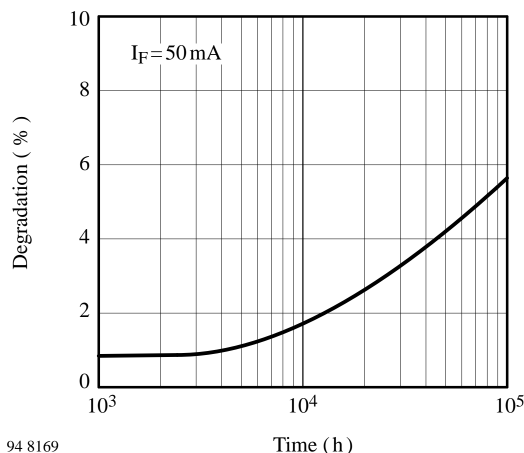

Figure 69. Average degradation of TSUS 5.

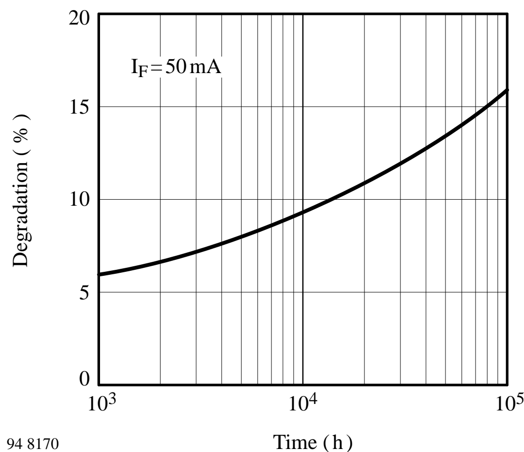

Figure 70. Average degradation of TSHA 5.

Safety

Reliability and Safety

All semiconductor devices have the potential of failing or degrading in ways that could impair the proper operation of safety systems. Well-known circuit techniques are available to protect against and minimize the effects of such occurrences. Examples of these techniques include redundant design, self-checking systems and other fail-safe techniques. Fault analysis of systems relating to safety is recommended. Environmental factors should be analyzed in all circuit designs, particularly in safety-related applications.

If the system analysis indicates the need for the highest degree of reliability in the component used, it is recommended that TEMIC be contacted for a customized reliability program.

Toxicity

Although gallium arsenide and gallium aluminium arsenide are both arsenic compounds, under normal use conditions they should be considered relatively benign. Both materials are listed by the 1980 NIOH ”Toxicology of Materials” with LD_{50} values (Lethal Dosis, probability 50%) comparable to common table salt.

Accidental electrical or mechanical damage to the devices should not affect the toxic hazard, so the units can be applied, handled, etc. as any other semiconductor device. Although the chips are small, chemically stable and protected by the device package, conditions that could break these crystalline compounds down into elements or other compounds should be avoided.

Safety Aspects of IR Radiation

Light and IR emitting diodes are included into the scope of the laser safety standards IEC 825 or EN 60825.

In the safety standard IEC 825–1 obviously the effects of extended sources are not or not correctly considered. The German standardization committee has proposed an amendment for the correction of the evident misinterpretations in June 1994.

The user of IR-transmission should be aware of the possible risks of retinal damage. Because of the errors inside the standard (editions of the year 1993) users should contact their national standardization committees to get the newest edition of the standard or, if it is not yet available, a statement for rating the potential of risk. The typical remote control and IrDA applications will not to be classified as a harmful application following the above mentioned German proposal.